6-1-2013

# A low-cost rice mapping remote sensing based algorithm

Ashraf Mohamed Abdelaziz Elshorbagy

The American University in Cairo

School of Sciences and Engineering

# A Low-Cost Rice Mapping Remote Sensing Based Algorithm

A Thesis Submitted to

Construction and Architecture Department

in partial fulfillment of the requirements for

the degree of Master of Science in Environmental Engineering

By

**Ashraf Mohamed Abdelaziz Elshorbagy**

Under the Supervision of:

Dr. Emad H. Imam

Professor, Department of Construction and Architecture Engineering, American University in Cairo

Dr. Mohamed H. Nour

Assistant Professor, Department of Construction and Architecture Engineering, American University in Cairo

May/2013

# DEDICATION

Praise be to God for giving me strength to finish this research. To my late father, I still miss you DAD and wish you were here. I learned from you a lot. You are my role model. May God bless your soul. To my wonderful mother, I wish you all the best in your life. Your prayers and continuous encouragement helped me finishing this research. To my great brothers, Mostafa, Ahmed and Mahmoud I do really love you all, from the bottom of my heart. I pray to God to give you a wonderful life. To my new family, my ever-beloved magnificent wife Eman, I cannot find the words to express how much I appreciate what you have done to me. You are my sunshine. To my daughter Lana, you are my princess; your smile reveals what so ever weariness I feel. To my uncle Nagi and Aunt Sal, I do really love you. To all my family especially aunt Magda and uncle Negm, I thank you for your continuous support.

# ACKNOWLEDGMENTS

To Dr. Emad, I do really appreciate your valuable comments and guidance throughout my thesis work. Thank you very much; I would not have made it without you.
To Dr. Nour, your comments and continuous encouragement is valued. I like you as a brother. Special thanks go to Dr.Rami, Dr. Hisham, Eng.Sanaa, Yasser and MIC staff. I would like to acknowledge the permission provided by the Canadian center for remote sensing in using the material in the background section and the permission provided by the satellite-imaging corporation to use some of their figures.

# Abstract

Egypt faces a great challenge, limited water resources and increasing water demand. The agriculture sector consumes about 83% of the available water resources. The main water-consuming crop planted in summer is rice. Thus for any better water resources management, rice mapping is required. Remote sensing can be utilized for rice mapping. This will potentially save money and effort. The most differentiating feature of rice is being flooded in the transplanting period. Xiao (2005) developed a rice mapping algorithm by studying the dynamics of three vegetation indices, the Land surface water index (LSWI), the normalized difference vegetation index (NDVI), and the Enhanced vegetation Index (EVI). The key assumption is that a moisture sensitive index, as LSWI, will capture the flooding of rice and will temporal lily exceeds or approaches NDVI, or EVI, thus signaling rice transplanting. Xiao utilized MODIS (500 m spatial resolution, twice a day temporal resolution) free satellite imagery. However, its coarse resolution combined with Egypt heterogeneous and fragmented land ownership raised the need for the algorithm modification.

In the current research a low-cost rice-mapping algorithm was developed. The accuracy of rice mapping from MODIS satellite imagery was enhanced by making use of LANDSAT imagery. This was achieved by developing a novel decision tree classifier that classifies land cover into its four main classes namely: vegetation, desert, bare land or urban, and water utilizing LANDSAT imagery. The non-vegetation area is then used to refine the rice area calculated from MODIS.

Another challenge of rice mapping from MODIS is that in rice fields the reflectance is a combination of water, vegetation, soil, and ditches thus not always the LSWI will exceed the EVI or the NDVI as proposed in the literature, but instead it will approach it in the transplanting period. In order to reflect this, a Δ-parameter was introduced. The adopted criteria for rice mapping was LSWI + Δ > NDVI or LSWI + Δ > EVI. The Δ-parameter was obtained as best fit for each rice-growing region. The Δ-parameter is different for EVI and NDVI. The Δ EVI for Kafrelsheikh and Dumyat was found to be 0.04. Daqehleya, Gharbeya and Sharqeya Δ-parameter was calculated as 0.05. While Behera governorate Δ-parameter was estimated to be 0.07. While Δ--NDVI parameter for KafrElsheikh was 0.174, for Dumyat was 0.178, for Sharqeya was 0.18, for Gharbeya was 0.197, for Behera was 0.23, and for Daqhleya the Δ- NDVI parameter was 0.155.

The developed rice-mapping algorithm was applied to the Delta region in Egypt to predict the rice cultivated areas in the year 2009. The resultant rice areas map was validated using randomly selected points, and local knowledge of rice planting practices, against very high-resolution (60 cm) imagery. The overall accuracy of the main land cover mapping was 90%. The rice areas map and probable transplanting dates conforms to local knowledge of rice planting practices. The results of this study indicate that the developed rice-mapping algorithm can be applied as an economic way for rice area mapping on a timely and frequent basis. However mapping rice fields prior to flooding would have been revealed more information for water management. More research should be directed to the early mapping of rice transplanting in the future.

## Table of Contents

## List of Tables

## List of Figures

# Chapter 1

# Introduction

## 1.1 Objectives

The main objective of this research is to develop a low-cost algorithm for rice mapping utilizing available free Satellite imagery, geographic information system (GIS) and field data. The specific objectives are:

- Explore the potential use of different satellite imagery products in rice mapping
- For the selected product, explore the potential use of literature-based vegetation indices in rice mapping
- Modify literature-based vegetation indicators to suit the Egyptian case study
- Develop rice mapping algorithms that rely on modified vegetation indices and ground-based information
- Calibrate the developed model using ground-based rice field samples for the year 2009 and 2010
- Validate the model with very high resolution imagery and other ground-based information
- Develop a comparative economic assessment for the selected mapping algorithm as compared to traditional supervised classification mapping approach

## 1.2 Definition of the Problem

Egypt share of water from river Nile is fixed with an annual amount of 55.5 billion $m^3$. In addition, with the population increase the per capita share of water rapidly decreased from nearly 2000 $m^3$/capita/year in 1959 to just 900 $m^3$/capita/year in 2000. Moreover, the problem is further complicated as it is predicted that the per capita share will be only 536 $m^3$/capita/year by year 2025 (AbdElhai, 2002). FAO defines the water poverty line as 1000m3/capita/year which signals that Egypt is classified as having a water poverty problem. The agriculture sector is the main water consumer in Egypt with an amount representing 83% of the available (CAPMAS, 2013).

Thus for better water resources management, the mapping of vegetation area is required. Rice is the most water-consuming crop planted in summer (Doss, 2001). Consequently, Rice is the most critical crop that should be mapped. Although accurate and timely information serve as the basis for any decision making process. Updated information about the vegetation area in Egypt and the rice fields planted is problematic. Every year the ministry of water resources and irrigation (MWRI) limits rice area to be planted in Egypt to 1.1 million feddan. This is to avail irrigation water to all agricultural land considering the limited water resources. In addition, this limit is related to the conveyance capacity of the irrigation network and its ability to satisfy the intense irrigation demands. Nevertheless, due to socioeconomic factors the farmers prefer to plant rice in their fields in violation of the MWRI regulations.

Every year the reported rice area is larger than that set by MWRI. In some years, the reported rice planted area is double the allowed. The extra rice planting area consumes

about 4 billion $m^3$ of water more than it would have been the case if another crop type like maize or cotton has been planted. This amount of excess water usage is equivalent to 4 billion $ of desalinated water, and accounts to nearly the current rate of water used for industry in Egypt (AQUASTAT FAO, 2013). Moreover, this excess amount represents about half that used for domestic purposes in Egypt.

Rice is the main water-consuming crop planted in the Delta. Thus rice mapping is essential for any water resources management improvement. The traditional methods like census and ground surveying are labor some, money and time consuming processes. On the other hand, remote sensing can provide a faster and updated mean for rice mapping. Mapping rice area can serve in building a spatial and temporal inventory of rice (where and when rice is planted). In addition, mapping rice area can be used in the determination of rice areas that are planted in violation of the MWRI regulations. An estimate of rice crop yield can be obtained from the rice area mapped. Knowing rice planting date for each rice area can help in the future planning of the delivery of the required irrigation water to rice areas especially in the most critical dates required.

### 1.3 Motivation

Identifying the cropland and crop types accurately on a large area scale with the traditional methods is uncertain. Remote sensing satellite images serve as a valuable source of data. Numerous studies since the seventies had shown that remote sensing is an ideal tool for vegetation mapping. The ongoing research continues to enhance the mapping accuracy. Feature extraction plays a significant role in correctly interpreting and extracting valuable information from the images. Various types of satellite images that

differ in their spatial, spectral and temporal characteristics can be used for vegetation mapping (Xie, 2008). Utilizing the technology of remote sensing is a practical and economical way to study the changes in the vegetation cover especially on large areas (Langely, 2001; Nordberg, 2003). Varying band combination and classification techniques affects the accuracy of portioning the space in the image to distinct classes. Cropping pattern is one of the important patterns to be identified and extracted accurately; to accomplish this task, feature extraction techniques are used. The spectral reflection of crops changes by crop type, phonology and health allowing it to be mapped and monitored by multispectral sensors. Rice mapping through remote sensing was conducted in several studies. Both radar and optical imagery were used for rice mapping in Turkey, Japan, Italy, China, Indonesia, and South East Asia. But due to the heterogeneous nature of the Egyptian cropping pattern, mapping rice in Egypt is a challenge. After reviewing the literature, no remote sensing based algorithm for rice mapping in Egypt that can utilize the imagery from the free domain and achieve high accuracy was found. Instead, the traditional method of rice areas reporting is doubtful. Accordingly developing a remote sensing based algorithm for rice mapping in Egypt will be of great importance; for better water resources management, planning and decision-making.

### 1.4 Approach in General

In order to develop an economic algorithm for rice mapping with high accuracy utilizing remote sensing and GIS, fine resolution imagery is used for arable area mapping. Frequent coarse resolution imagery is used for rice area mapping by examining the dynamics of vegetation and other remote sensing driven indices with a small number of

intelligently selected training samples. The blending of fine resolution imagery arable area mapping and the coarse resolution imagery rice area mapping is applied. Very high-resolution imagery (60 cm), field data and knowledge of rice planting practices will be used for the validation of the rice mapping algorithm. The developed algorithm will be applied for rice area mapping in each main rice-planting governorate in Egypt. The adjustment of the vegetation and moisture driven indices analysis will be carried out for each main rice-planting governorate. The effect of arable area tuning for each governorate will be calculated.

## 1.5 Thesis organization

The remainder of the thesis is as follows:

1- Chapter Two provides a basic background about remote sensing, the application of remote sensing for land types classification and the work of other researchers for rice mapping from remote sensing.
2- Chapter three presents the development of the remote sensing based algorithm for rice mapping.
3- Chapter four presents the application of the developed algorithm for rice mapping in Egypt delta governorates.
4- Chapter five provides a feasibility study of potential satellite imagery that can be used for rice mapping in Egypt Delta with traditional supervised classification approach, the key advantages of the developed rice mapping algorithm
5- Chapter six presents the summary, conclusions and findings of this research as well as the recommendation for future research

# Chapter 2

# Background and Literature review

## 2.1 Background:

### 2.1.1 Remote Sensing by Satellite Imagery

Egypt faces a great challenge; limited water resources and increasing water demand due to population increase. The agriculture sector consumes about 83% of Egypt water resources (CAPMAS, 2013). Thus, efficiency in managing the water resources usage in the agriculture sector is of great importance. Identifying the cropping pattern in an accurate way helps better managing the available water resources. Rice is the most water-consuming crop planted in summer. One feddan of rice consumes about three times the amount of water consumed by maize (Doss, 2001). Thus, rice field mapping is very important for better water resources management.

The traditional methods of rice field mapping are ground surveying and from census, which both are not up to date, time consuming, money and labor effort intensive processes. On the other hand, remote sensing can be used effectively to map rice fields and monitor rice crop dynamics (Cheng et al., 2004).

Remote sensing is defined by Canada center for remote sensing as "Remote sensing is the science (and to some extent, art) of acquiring information about the Earth's surface without actually being in contact with it. This is done by sensing and recording reflected or emitted energy and processing, analyzing, and applying that information."

Remote sensing involves seven basic elements (A) until (G) (The Canadian center of remote sensing) as illustrated in Fig 2.1. The first element is the source of energy (A) which illuminates the target. The second element is the radiation and interaction of energy with the atmosphere (B) while travelling from the source to the target and in its way from the target to the sensor. The third element is the interaction of the energy with the target (C) which depends on the target and the type of radiation. The fourth element is the remotely located sensor (D) that records the energy reflected or emitted from the target. The fifth element is transmission reception and processing (E) where the recorded energy by the sensor is transmitted to a receiving station where the data received is processed into an image. The sixth element is the image interpretation and analysis (F) where the image is interpreted visually or electronically to extract information about the target which was illuminated. The seventh and last element of the remote sensing process is the application (G) of the extracted information achieved when the extracted information is used for better understanding of the target or for decision-making.

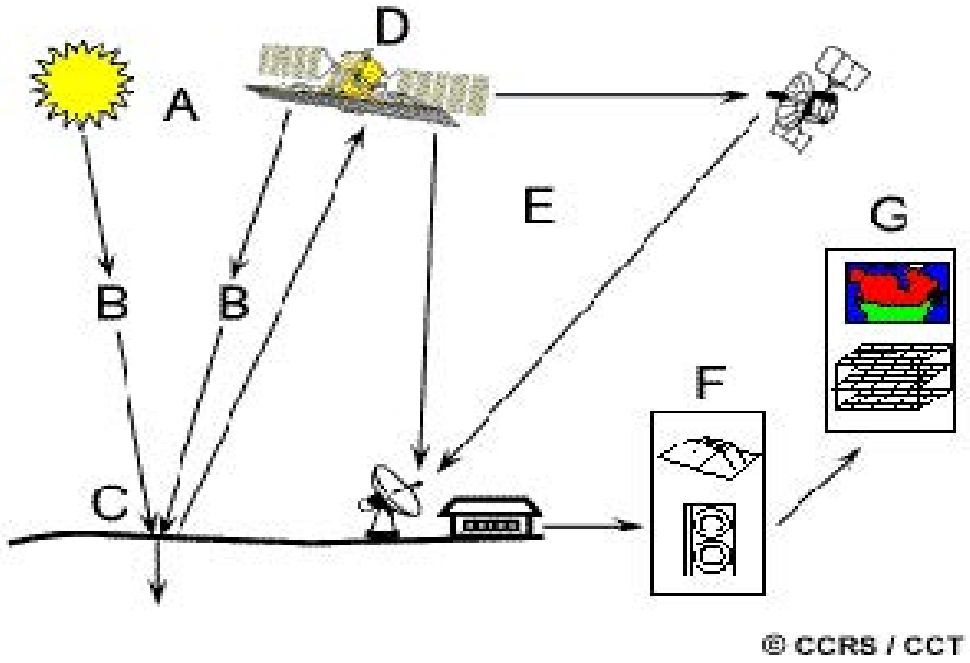


Fig 2-1: Elements of the remote sensing (After the Canadian Center of Remote sensing, 2013)

The satellites used in remote sensing for earth observation can be either active or passive. This depends on the source of energy used for illuminating the sensed targets. The passive satellites depend on the sun as the source of electromagnetic waves that illuminate the sensed targets. On the other hand, the active satellites as radars are themselves the sources of energy produced to illuminate the sensed targets. Conventional active satellites transmit and receive horizontally polarized electromagnetic waves (HH) while dual-polarization transmits and receives pulses that are polarized both horizontally and vertically (VV-HH). The main advantage of the active satellites is that they are all weather conditions imaging instruments. This means that they can penetrate clouds and image the targets. Nevertheless, their drawback is that it is not easy to handle radar imagery. In addition the wind and topographic conditions may affect the measured

energy. Measuring the amount of energy reflected or emitted from the sensed targets by the satellites can provide a wealth of information.

### 2.1.2 Satellite Imagery Resolutions

Satellite images used in remote sensing vary in their temporal, spectral and spatial resolution. The resolution of an image refers to the potential detail that it can provide. Temporal resolution refers to how frequent the satellite can image the same area. Spectral resolution refers to the specific wavelengths in the electromagnetic spectrum that the satellite can record. Spatial resolution refers to the smallest target size that can be detected by the satellite.

#### 2.1.2.1 Temporal resolution

Temporal resolution means the revisit time of the satellite to be able to image the same area on earth again. They vary from twice a day to several days or even weeks. This depends on the sensor orbit, altitude, viewing angle, and on the target location. Fig 2.2 illustrates the temporal resolution of a high resolution satellite(IKONOS). From this figure we can deduce that for a target on the equator to be sensed with a 1m spatial resolution the revisit time will be about 4 days. On the other hand, if the target is on latitude 75 then the revisit time will be as short as 0.5 days to be sensed with the same 1m

spatial resolution.

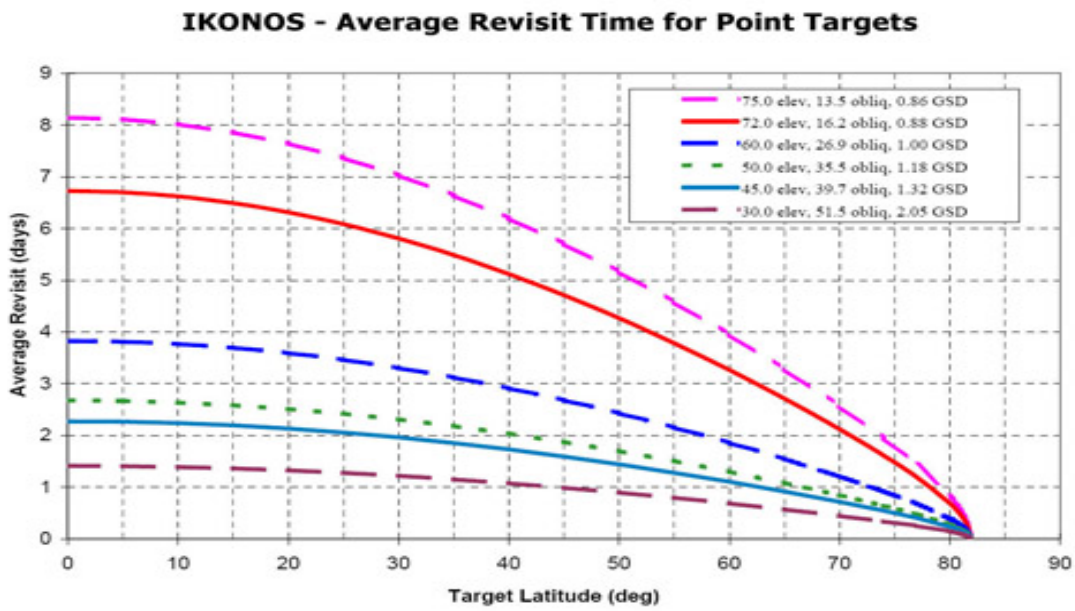


Fig 2-2: IKONOS revisit time (After Satellite Imaging Corporation, 2013)

#### 2.1.2.2 Spectral Resolution

The spectral resolution means the wavelengths in the electromagnetic spectrum that the satellite can record as can be shown in Figs 2-3 and 2-4. Fig 2-3 shows the visible bands that can be sensed by our eyes, which range in their wavelength from about 400 nm to about 700 nm. In Fig 2-4, the bands that can be sensed by the ASTER and LANDSAT satellites are shown. LANDSAT TM satellite records energy in the visible bands(bands 1,2,3) ; near infra-red bands NIR (band4) ; short wave infra-red SWIR (bands 5,7) ; thermal infra-red TIR(band6). LANDSAT TM bands characteristics can be summarized in table 2.1. The ASTER satellite records energy in the visible bands( bands 1,2); NIR(band3) ; SWIR (bands 4,5,6,7,8,9); TIR (bands 10,11,12,13,14). Table 2.2 summarizes ASTER bands characteristics.  The satellites vary in their spectral resolution

from few bands like in multispectral sensors to hundreds of bands like the hyper spectral sensors.

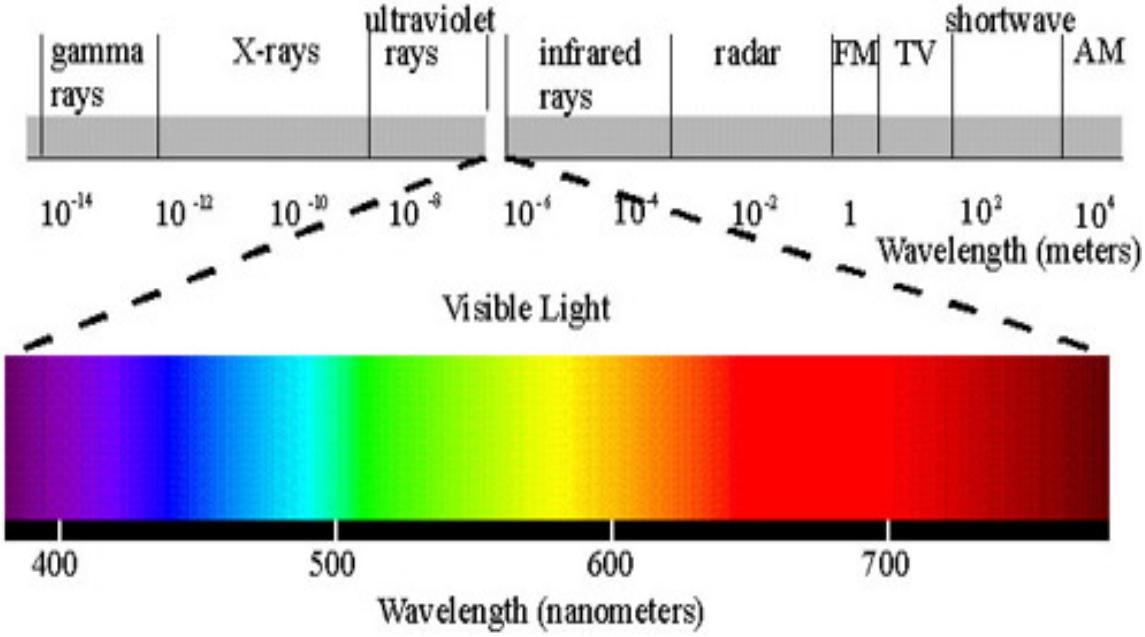


Fig 2-3: Visible wavelength recorded by satellite (After Satellite Imaging Corporation, 2013)

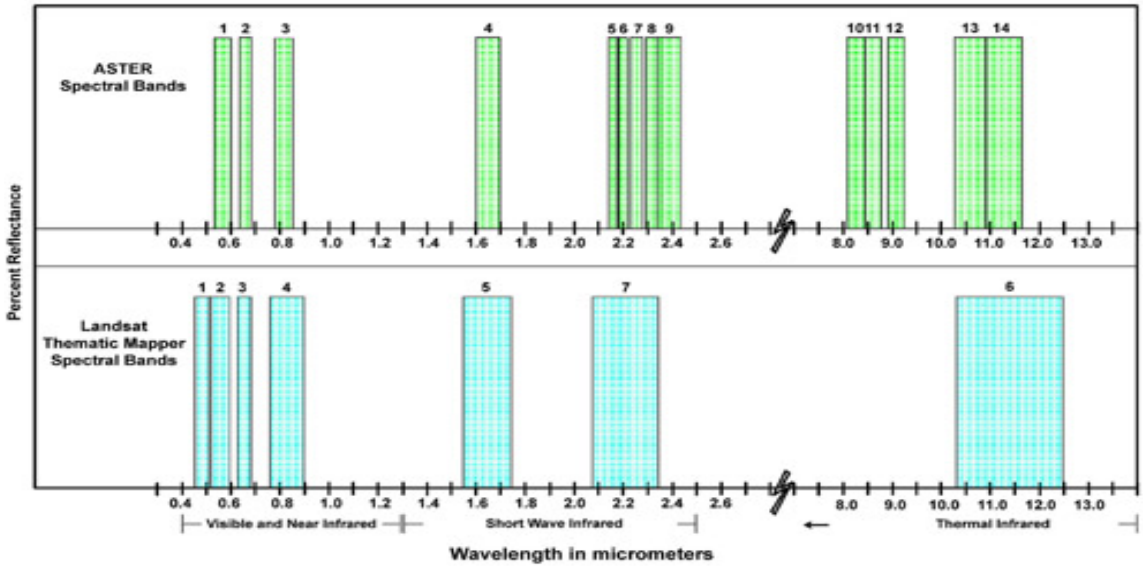


Fig 2-4: ASTER and LANDSAT bands(After Satellite Imaging Corporation, 2013)

Table 2-1: LANDSAT TM bands

| **Band** | **Band No.** | **Spectral Range (µm)** |
|---|---|---|
| Visible | 1 | 0.45-0.52 |
| | 2 | 0.52-0.60 |
| | 3 | 0.63-0.69 |
| NIR | 4 | 0.76-0.90 |
| SWIR | 5 | 1.55-1.75 |
| TIR | 6 | 10.40-12.50 |
| SWIR | 7 | 2.08-2.35 |

Table 2-2: ASTER bands

| Band | Band No. | Spectral Range (µm) |
|---|---|---|
| Visible | 1 | 0.52-0.60 |
| | 2 | 0.63-0.69 |
| NIR | 3 | 0.78-0.86 |
| SWIR | 4 | 1.60-1.70 |
| | 5 | 2.145-2.185 |
| | 6 | 2.185-2.225 |
| | 7 | 2.235-2.285 |
| | 8 | 2.295-2.365 |
| | 9 | 2.360-2.430 |
| TIR | 10 | 8.125-8.475 |
| | 11 | 8.475-8.825 |
| | 12 | 8.925-9.275 |
| | 13 | 10.25-10.95 |
| | 14 | 10.95-11.65 |

#### 2.1.2.3 Spatial Resolution

The spatial resolution reflects the minimum detectable target size that the sensor can record. As the satellite is higher in the altitude (Far from the targets) the spatial resolution is coarser but the width the satellite can observe is wider (swath width). On the other hand for the satellite to have a fine spatial resolution its altitude is lower (near from the targets) but its swath width decreases. Thus, the recorded reflectance within the spatial resolution will be the averaging of the targets present within that area. The spatial resolution of the available commercial satellites varies from few kilometers to 50 cm. As the spatial resolution gets coarser, the effect of averaging will be bigger as it is shown in Figs 2-5 and 2-6.

In Fig 2.5, as the spatial resolution gets finer the blue house can be accurately mapped. For a 30m spatial resolution the blue house will be displayed as if covering the whole pixel area. Thus the extent and house area will be overestimated. While for the finer spatial resolution 1m the actual extent and area of the blue house is better mapped.

In Fig 2.6, some different combination of land types occurs in each pixel of the satellite image. The mapping of land types in each pixel will depend on the spatial resolution of the satellite. For example, in pixel 2, building and vegetation occur but the whole pixel will be mapped with remote sensing (RS) as building thus overestimating the building area and underestimating the vegetation area. In pixel 3, the opposite occur, as the whole pixel will be mapped as vegetation thus overestimating vegetation area and underestimating building area.

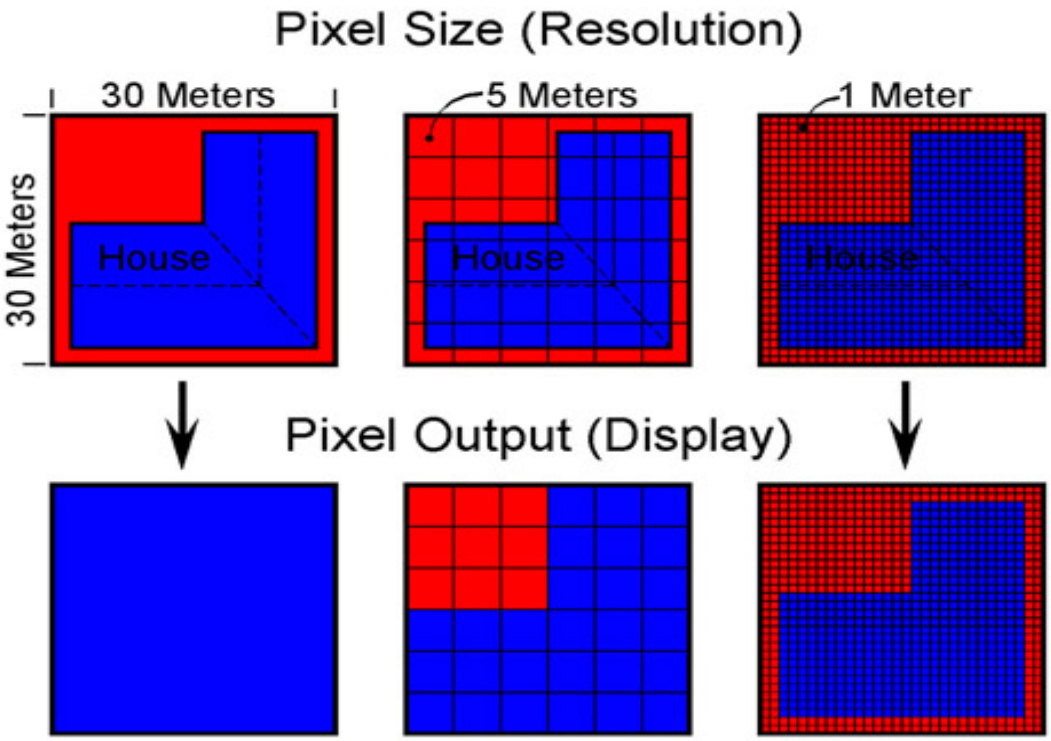


Fig 2-5:Effect of Pixel Spatial Resolution on Mapping (After Satellite Imaging Corporation, 2013)


Fig 2-6: Spatial Resolution and Averaging

The spatial resolution effect on the information that can be interpreted and extracted from the satellite image of Fig 2-6 is summarized in Table 2-3.

Table 2-3: Summary of spatial resolution effect on the information extracted by remote sensing (RS)

| | Pixel 1 | Pixel 2 | Pixel 3 | Pixel 4 |
|---|---|---|---|---|
| Rs output | Vegetation first type(brown) | Non vegetation | Vegetation | Vegetation second type(green) |
| Actual land cover | Vegetation | Vegetation + building | Vegetation + building | Vegetation |
| Errors | Two types of vegetation but mapped as one type | Vegetation not mapped | Building not mapped | Two types of vegetation but mapped as one type |

### 2.1.3 Some Common Satellites characteristics

Several satellites orbit the earth; acquire imagery and make them available to potential users. The most commons are MODIS, LANDSAT TM, SPOT 5, RAPIDEYE and WORLDVIEW2. These satellites differ in their spatial, spectral, temporal resolution and the swath width. In addition the cost of obtaining the imagery from these satellites differs from obtaining the imagery free of charge like the case with the MODIS satellite and about 40$/Km$^2$ for the WORLDVIEW2 satellite. The main characteristics of these satellites are summarized in Table 2-4.

The selection of the satellite imagery to be used for extracting information depends on the application, the required accuracy and the budget available. One should make a compromise between the spatial, spectral, and temporal resolution that are required for the application under consideration. For example the WORLDVIEW2 images have the highest spatial resolution but they are the most expensive. In addition, their swath width is the smallest which requires many scenes to cover the same area that could be covered by one scene of MODIS or LANDSATTM.

Table 2-4: Main Characteristics of Commercial Satellites

| Satellite Name | Category | Bands | Band Name | Bandwidth (nm) | Spatial Resolution (m) | Scene dimensions (Km) | Revisit time (days) |
|---|---|---|---|---|---|---|---|
| MODIS | Coarse resolution | | | | | 1100 *1100 | Twice per day (Terra, Aqua) |
| | | 1 | Red | 620 - 670 | 250 | | |
| | | 2 | Near Infra Red (NIR) | 841 - 876 | 250 | | |
| | | 3 | Blue | 459 - 479 | 500 | | |
| | | 4 | Green | 545 - 565 | 500 | | |
| | | 5 | Short Wave Infra Red (SWIR 1) | 1230 - 1250 | 500 | | |
| | | 6 | Short Wave Infra Red (SWIR 2) | 1628 - 1652 | 500 | | |
| | | 7 | Mid Infra Red (MIR) | 2105 - 2155 | 500 | | |
| Landsat | Mid resolution | | | | | 170 km north-south by 185 km east-west | 16 days |
| | | 1 | Blue | 450-520 | 30 | | |
| | | 2 | Green | 520-600 | 30 | | |
| | | 3 | Red | 630-690 | 30 | | |
| | | 4 | Near Infra Red | 760-900 | 30 | | |
| | | 5 | SWIR 1 | 1550-1750 | 30 | | |
| | | 6 | Thermal | 10400-12500 | 120 | | |
| | | 7 | Mid Infra Red (MIR) | 2080-2350 | 30 | | |
| | | | | | | | |
| SPOT | Mid resolution | | | | | 60*60 | 2-3 days |
| | | 1 | SWIR | 1580-1750 | 10 | | |
| | | 2 | NIR | 780-890 | 10 | | |
| | | 3 | RED | 610-680 | 10 | | |
| | | 4 | Green | 500-590 | 10 | | |
| | | | | | | | |
| Rapideye | Mid resolution | | | | | 24*24 area based | Daily |
| | | 1 | Blue | 440-510 | 5 | | |
| | | 2 | Green | 520-590 | 5 | | |
| | | 3 | Red | 630-685 | 5 | | |
| | | 4 | Red Edge | 690-730 | 5 | | |
| | | 5 | NIR | 760-850 | 5 | | |
| | | | | | | | |
| Worldview 2 | Very high resolution | | | | | 16.4*16.4 area based | 1-4 days |
| | | 1 | Coastal | 400-450 | 2 | | |
| | | 2 | Blue | 450-510 | 2 | | |
| | | 3 | Green | 510-580 | 2 | | |
| | | 4 | Yellow | 585-625 | 2 | | |
| | | 5 | Red | 630-690 | 2 | | |
| | | 6 | Red Edge | 705-745 | 2 | | |
| | | 7 | Near - IR 1 | 770-895 | 2 | | |
| | | 8 | Near - IR 2 | 860-1040 | 2 | | |

### 2.1.4 Remote sensing and land cover

Remote sensing was used from the seventies to extract information about land cover and land use. Land cover describes the physical land type that covers the earth like water , forest or urban areas while land use document the way people uses this land cover for example recreation, wildlife habitat and residential. Remote sensing extracted information is mainly linked with land cover but with the help of ancillary data land use can be mapped. Each land type interacts differently when illuminated with electromagnetic waves. The response of the land type to each wavelength differs. This depends mainly on the chemical and physical properties of the land type. The percent of the electromagnetic energy reflected by each land cover differs according to the wavelength. By studying this response for known land types one can predict the land type from its distinct spectral response.

Fig 2-7 shows the typical response curve for some land covers. The percentage reflectance (vertical axis) of the electromagnetic waves differs from one land cover to another according to the electromagnetic wavelength (horizontal axis). As can be seen the pattern of reflectance differs for vegetation, water and bare soil. The different response pattern can be used for classification. The most distinguishing feature of vegetation pattern is the sudden peak in the NIR reflectance compared to the reflectance in the Red wavelength which can easily differentiate vegetation from water and bare soil land covers. While water pattern most distinguishing feature is the very low reflectance starting from the NIR wavelength. For the soil pattern most distinguishing feature is the almost steady increase in the reflectance as the wavelength increases.

Fig 2-8 shows the typical spectral response curves for some land types and the LANDSAT TM satellite bands.

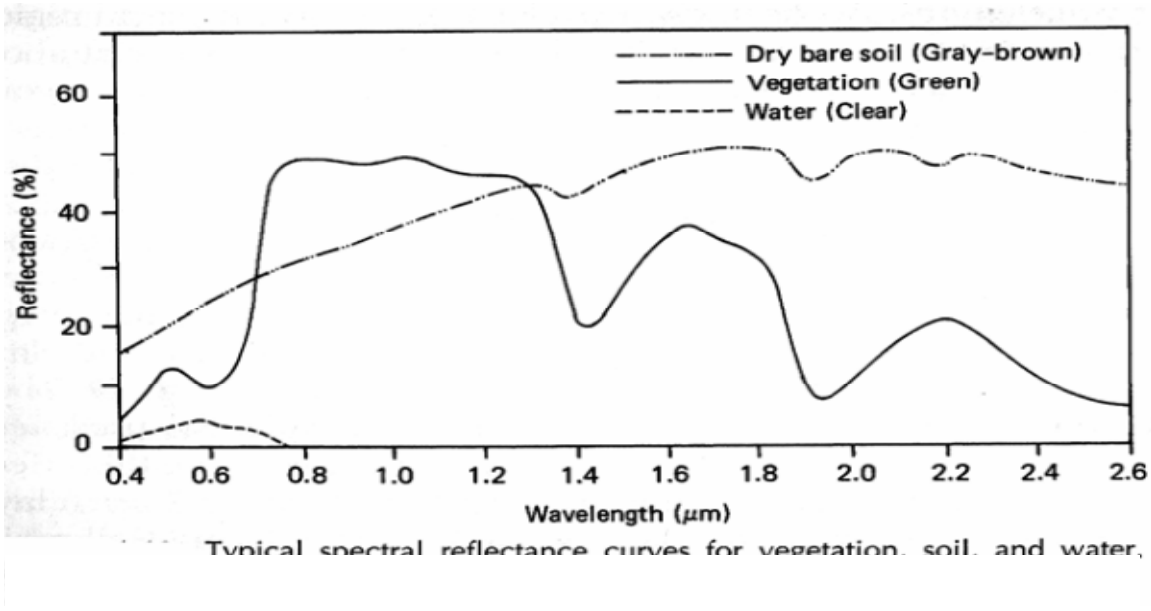


Fig 2-7: Typical spectral reflectance curves for vegetation, soil, and water. (Adapted from Swain and Davis, 1978)

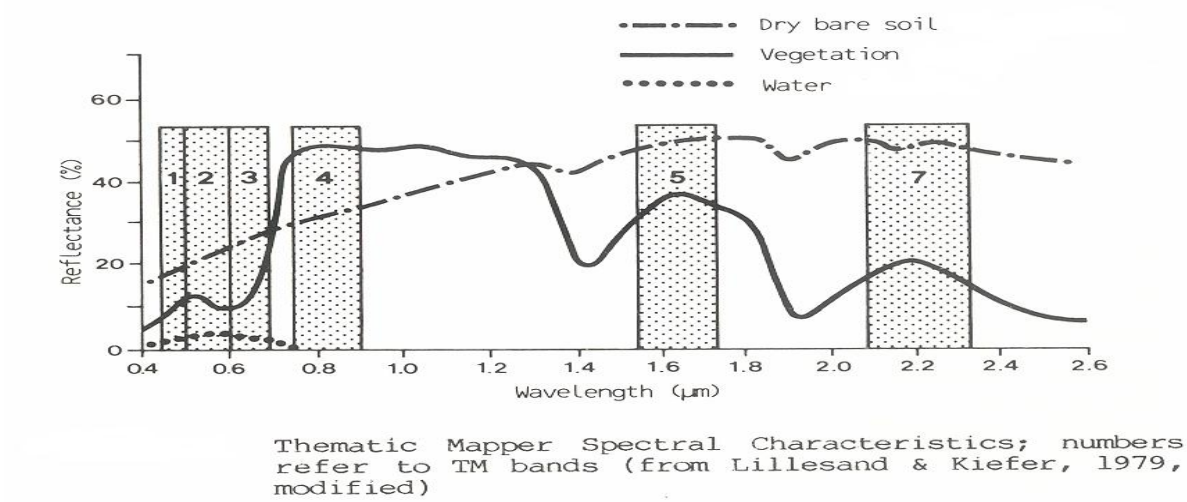


Fig 2-8: Thematic Mapper Spectral Characteristics; numbers refer to TM bands (from Lillesand and Kiefer, 1979)

### 2.1.5 Some Common Vegetation Indices

The vegetation indices (VI) depend on the vegetation reflectance pattern where there is a sudden peak in the NIR reflectance compared to the Red wavelength reflectance. Combining the red and NIR wavelengths a variety of VI were developed. The most frequently used is the normalized difference vegetation index (NDVI).

**NDVI = (NIR- Red) / (NIR + Red)**

Where

NIR = the near infra-red band reflectance (841-876 nm)

Red=the red band reflectance (620-670 nm)

The NDVI ranges from -1 to 1. Healthy vegetation NDVI value is in the range of 0.5-0.9. While water bodies have very low or negative NDVI values.

The enhanced vegetation index (EVI) is a modification of the NDVI to correct for some distortions caused by atmospheric interaction as well as the ground cover under vegetation.

**EVI = 2.5*(NIR - RED/ (NIR + 6 * RED -7.5* BLUE + 10000))**

Where

NIR = the near infra-red band (841-876 nm)

Red=the red band (620-670 nm)

Blue= the blue band(459-479 nm)

Another developed index that is sensitive to vegetation water content is the land surface water index (LSWI). Unlike NDVI, EVI which changes in response to vegetation greenness the LSWI changes in response to vegetation moisture. LSWI is calculated as follows

**LSWI = (NIR- SWIR) / (NIR+ SWIR)**

Where

NIR = the near infra-red band (841-876 nm)

SWIR=the short wave infra-red band (1628-1652 nm)

### 2.1.6 Satellite Imagery Classification Methods

The methods used to classify the satellite imagery into land types can broadly be grouped under supervised or unsupervised classification. In the supervised classification, the priori knowledge of land types present is required. The collection of representative training samples of each type is essential. These samples are then used to train the chosen classifier. By applying some set of classification rules (depending on the classifier used), each other pixel in the satellite image is classified accordingly. On the other hand, the unsupervised classification depends mainly on the natural grouping of the image pixels according to their spectral properties. The priori knowledge of the land types present is not required. Unsupervised classification is similar to cluster analysis. The user is required to specify basic information such as which bands to be used and the number of the clusters. The user then assigns to every outputted cluster a meaningful label. In addition, the user may have to group or split some clusters to represent the interested land type. The main traditional methods of the image classification are; the classical K-mean or ISODATA in the unsupervised classification, or the maximum likelihood classifier (MLC) in the supervised classification. In the MLC a Bayesian probability function is calculated based on statistics (mean; variance/covariance) from the training sites. For each other pixel it is judged as to the class to which it most probably belongs.

One of the important land covers to be mapped is vegetation. Mapping vegetation area is very important for planning and resources management. Remote sensing can provide a very useful tool that helps accomplish this task. Mapping vegetation utilizing remote sensing was and still an active research topic. Researches have been attempting to improve the classifiers used in terms of increasing the accuracy of the mapping.

The unsupervised classification is a straightforward process but it has to be repeated again if new data is added. In addition, the assigning of the classes after the classification process is not applicable for the vegetation species discrimination (XIE, 2008). On the other hand, the most widely used supervised classifier is the maximum likelihood MLC that depends on the statistical distribution of the satellite image (Langely, 2001; Nordberg, 2003). This dependency on the statistical distribution results in less satisfactory results if the data does not follow a Gaussian distribution. Moreover, a well-defined training samples collection plan is required to collect the essential training samples for the classifier, which is not an easy task.

One of the most important crops to be mapped is Rice. This is because rice is one of the most water consuming crops. For example, the main crops that are planted in Egypt delta in summer are rice, maize, and cotton. Rice consumes about 6500 m3/feddan while maize consumes 2400 m3/feddan, and cotton consumes 2600 m3/feddan (Doss, 2001). Thus for any better water resources management rice mapping is required.

### 2.1.7 Rice (Oryza Sativa)Crop

Rice has four planting phases: i) pre-planting, ii) vegetative, iii) reproductive, and iv) ripening phase (IRRI, 2013).

In the Pre planting phase the farmer, select the well-adapted rice variety and good quality seeds and prepare the land by flooding which consumes more than one third of the rice water requirements.

The vegetative phase starts by seed establishment and ends at the panicle initiation. During this phase there is continuous ponding of water of about 5 cm depth which lasts for about 55 days in a 120 day rice variety

The Reproductive phase extends from panicle initiation to flowering and usually lasts for 35 days. In order to maintain good yield water depth in fields must be kept at about 5 cm in all times.

The final Ripening phase extends from flowering to maturing and usually takes 30 days when submersion is not required as soil with 80-90% saturation is sufficient. The fields are then drained 10-15 days before the expected harvesting date

In this research a rice-mapping algorithm for Egypt was developed. Where it make use of the freely available MODIS imagery and blending it with the finer LANDSAT TM 30 m imagery trying to make use of the advantages of MODIS imagery and minimizing its mixed pixel shortcoming. The next chapter elaborates the developed rice-mapping algorithm.

## 2.2 Literature review:

Since different vegetation types have similar spectra reflection, and that the reflection of the same crop type may differ from place to place depending on many factors like the phonology, crop health, and soil moisture therefore accurately classifying satellite images is problematic with the traditional classifiers (the K-mean or MLC). The focus of research on trying to find better classifiers is an ongoing process. There was great progress in developing powerful classifiers to extract vegetation covers from remote sensing images (XIE, 2008).

Several studies have utilized remote sensing for rice fields mapping. Different satellite images and mapping algorithms were used. These studies can be categorized according to the type of imagery used and whether they are from active (radar imagery) or passive satellites (optical imagery). A brief description of these studies is as follows.

ERS-1 radar images were used by Chakraborty in 1997 to map rice fields grown under different cultural practices in India. Chakraborty developed an artificial neural network for mapping rice fields from three images during the rice growing cycle (Chakraborty, 1997). The temporal variation of rice backscattering during its growing cycle was used for rice mapping. Unlike optical imagery, radar image is formed through the coherent interaction of the transmitted microwave with the targets. Therefore, it suffers from the effect of speckle noise which arises from the coherent summation of the signals scattered from ground scatterers (CRISP, 2001). In addition, wind and topographic effect could affect the backscatter coefficients thus hindering the usefulness

of the data. In order to prepare the data for analysis and remove this noise some sophisticated techniques are required. Thus the utilization of radar imagery is not easy.

Backscatter change index (BSCI) was developed for rice mapping in China using ENVISAT/ASAR data. The dual polarization VV and HH of ENVISAT/ASAR in two dates during rice growing cycle were used to discriminate rice fields from other land types (Wang et al., 2008). The backscatter change index was calculated combining the VV and HH backscatters of the two dates. It was found that the value of (BSCI) is much higher for the rice fields than other land covers. Producer's accuracy of about 80 % and user accuracy of about 90% was achieved (Wang et al., 2008).

Bouvert also used the dual polarization of ENVISAT/ASAR imagery for rice mapping in Mekong delta Vietnam (2009). A prior statistical study of the polarization ratio of HH/VV for rice and non-rice pixels at different dates was performed. The difference in the ratio HH/VV for rice and non-rice fields was then used for rice mapping. A 90% overall accuracy was reported. But Bouvert pointed out the need for relevant speckle filtering prior to classification (2009).

An object-oriented classifier was developed using six scenes of ENVISAT/ASAR images covering Fuzhou area in China to map rice fields and 90% classification accuracy for rice was reported (Ling, 2005). Instead of doing the classification on a pixel based system Ling applied a soft classifier that depends on fuzzy logic applied on image segments as the basic processing units.

ALOS/PALSAR radar imagery was used to map rice fields in Zhejiang Province, southeast China (Yuan, 2009). In the mapping algorithm Yuan used three images in three

dates (at the begging, middle, and end of rice planting season) and with the help of training samples the backscatter coefficients of rice had been pinpointed. These coefficients were then applied in a Support Vector Machine (SVM) classifier to map rice. A user and producer accuracy of 90% and 76% respectively were reported (Yuan, 2009).

Ozkuralphi examined multi-temporal Radarsat1 imagery to map rice fields in Turkey by developing a time dependent radar backscatter curve (2007). Multi-date images were then used with the maximum likelihood classifier to map rice fields. 91% overall accuracy of rice mapping was achieved.

These studies made use of the main radar imaging advantage, that it is all weather imaging sensors. This is very important in the areas where there is almost persistent cloud cover all year around. However, the common drawback in these studies is that the utilization of radar imagery is not easy and requires some sophisticated techniques to obtain satisfactory results (Wang, 2008). Another common issue with the radar imagery is that wind and topographic effect could affect the backscatter coefficients and the case of scattering from wet vegetation is further complicated (Hobbs, 1998).

Optical imagery was also used for rice mapping. Both fine resolution imagery like LANDSAT (30 m resolution) and moderate resolution imagery like AVHRR (1 km resolution) were used for rice fields mapping. The usage of fine resolution imagery were mainly assigned with applying image classification procedures while the usage of moderate resolution imagery were primarily based on studying the temporal development of the normalized difference vegetation index (NDVI) (Xiao, 2005). The availability of moderate resolution imagery free of charge and its fine temporal resolution attracted

several researches to utilize them in rice mapping. The launch of MODIS in 2002 with its 250 m spatial resolution in the red and near infrared bands and its daily revisit capability made it the preferable moderate resolution alternative for mapping rice.

Cheng utilized rice-training samples to classify two MODIS imagery (at the beginning and at the end of the rice growing cycle) using the supervised minimum distance classifier and enhancing the classification with GIS layers of irrigated and rain fed agriculture areas. The GIS layers were used to mask potential rice fields (2004). By introducing another source of information like the GIS layers, he was able to decrease the misclassification errors. Comparing the total rice area against agricultural bureau area Cheng reported 95% rice classification accuracy.

Boschetti was able to monitor rice crop phonology in Italy through time series analysis of 5 years (2001-2005) of MODIS imagery. Where MODIS NDVI 16 days product was used to extract rice phonological stages through the analysis of NDVI profile (2009).

Sakamoto was able to determine rice-planting, heading and harvesting dates for rice in Japan through studying the smoothed profile of enhanced vegetation index (EVI) extracted from MODIS/TERA imagery. The smoothed profile of EVI was necessary before phonological stages can be determined (2005).

Xiao introduced a novel algorithm for rice mapping through temporal profile analysis of Land Surface Water Index (LSWI) and NDVI extracted from SPOT VEGETATION imagery (1km spatial resolution, 10 days temporal resolution). He made use of the most differentiating feature of rice, which is that rice transplanting occurs on

flooded soil. The LSWI was sensitive enough to capture the temporal increase in soil moisture during rice transplanting. Thus, LSWI temporarily exceed NDVI (2002). The algorithm was modified by including EVI in the temporal profile analysis and utilizing MODIS imagery (500m resolution, 8 days temporal resolution) (Xiao, 2005). The algorithm was then used to map rice fields in South East Asia (Xiao, 2006). Modification of the algorithm to further classifying rice paddies in South East Asia according to the ecosystem by slope of the Digital Elevation Model (DEM) analysis and urban masking was done (Bridhikitti, 2012). Another modification of the algorithm by making use of the rice-planting calendar and using threshold for the indices LSWI, EVI, NDVI from known rice fields and smoothing of NDVI,EVI was used to map rice in China ( Sun, 2009). But the usage of threshold values could be critical when applied in other environment (Boschetti, 2009).

The common drawback of the above-mentioned studies is the usage of MODIS imagery with the 500 m resolution introducing the mixed pixel dilemma especially in heterogeneous environments as illustrated in Fig 2-9.

Fig 2-9 shows an area in Kafrelsheikh where different mixed features depending on the pixel size of the satellite image can be seen. This is overlaid over a 2m Worldview2 image. The MODIS pixel with a 500 m resolution will be the averaging of vegetation, urban, water and roads. Likewise, as the spatial resolution is finer the less averaging will occur as can be seen in the SPOT pixel with 10 m resolution.


Fig 2-9: Mixed features within a pixel spatial resolution

Okamato tried to combine both radar and optical imagery for mapping newly rice-planted areas in Indonesia. Farmers in this study area are able to plant rice all over the year if there is sufficient water. This rice cultivation method is indigenous to tropical regions. The unsupervised classification of LANDSAT TM data acquired in the dry season was used to map the arable land while the JERS-1 radar imagery was used to map submerged lands in the rainy season. With the aid of local rice-planting calendar and practices, he was able to identify, new rice fields planted which satisfies both conditions of being arable land and submerged (1998).

# Chapter 3

# The Rice Mapping Algorithm

## 3.1 Rice mapping Algorithm

In this research a rice-mapping algorithm for Egypt Delta will be developed. The freely available MODIS imagery 500m and the finer LANDSAT TM 30 m imagery will be utilized. The combination between LANDSAT TM and MODIS imagery in the algorithm will benefit from MODIS imagery fine temporal resolution and minimizing its mixed pixel shortcoming with the usage of LANDSAT TM fine spatial resolution.

Vegetation versus non-vegetation areas mapping module (veg-non-veg) will be implemented. This will make use of LANDSAT TM fine resolution (30 m) satellite imagery (in June 2013 the new LANDSAT 8 ( 30 m) freely available imagery could also be used) and the different response curves for the main Delta land types; namely vegetation, urban or bare land, desert and water. In the veg-non-veg module, a decision tree classifier will be constructed. The four key land covers: water, vegetation, desert and urban areas will be classified. In order to classify these key land covers with high accuracy images with finer spatial resolution will be used. The module will be applied on two or more images in different seasons while the vegetation lands are cultivated. The vegetation areas will then be used to tune the mapping of rice areas.

The suitability of using vegetation and other remote sensing driven indices with a small number of intelligently selected training samples to map rice fields economically will be examined.

The main differentiating feature of rice from other crops is that it is flooded during the transplanting period. The dynamics of vegetation and moisture driven indices will be affected by this physical phenomenon. However, due to the 16 days LANDSAT TM revisit time it may miss these dynamics. MODIS freely available imagery (500 m resolution) with its frequent revisit time (Twice a day) provides a wealth of information that is used for vegetation and moisture indices calculation. Rice planting calendar in Egypt is used to select the imagery dates for MODIS imagery to be acquired. By analyzing the dynamics of vegetation and moisture driven indices that is adapted for each main rice-planting governorate, the rice area will be mapped. Cloud, permanent water bodies, and local knowledge of rice transplanting dates all will be used for rice area mapping correction.

The blending of LANDSAT TM analysis to map vegetation areas -that is validated by 1000 randomly selected points against very high-resolution imagery (60 cm) - with the MODIS vegetation and moisture driven indices analysis will result in a feasible remote sensing based algorithm for rice mapping in Egypt. The developed algorithm will be applied for rice area mapping in each main rice-planting governorate. The effect of LANDSAT TM tuning for each governorate will be calculated. In addition, the adaptation of the vegetation and moisture driven indices analysis for each main rice-planting governorate will be highlighted. The next sections elaborate the developed rice-mapping algorithm.

Taking advantage of the main differentiating feature of rice (it is flooded during the transplanting period) in the mapping process could be achieved by examining the relation between a water sensitive index, the Land Surface Water Index (LSWI) and

vegetation index (Normalized Difference Vegetation Index NDVI or Enhanced Vegetation Index EVI). The MODIS series of imagery during the rice-planting period are utilized for LSWI, NDVI, and EVI calculation. The relation between the three indices for each pixel is examined. The assumption is that when the rice is flooded in the transplanting period; the LSWI will exceed or approach NDVI or EVI due to the presence of water. Afterwards the rice plant will continue to grow covering the water and thus the vegetation indices will be greater than the LSWI. Thus when LSWI > EVI or LSWI> NDVI this signals the flooding of the fields.

MODIS satellite imagery is a valuable source of information. Its capability of acquiring daily images with resolutions 250m, 500m, and 1km for the different bands and being free of charge can help in vegetation mapping and monitoring. MODIS images are used for rice mapping by studying multi temporal imagery during the planting season. The MODIS Terra/Aqua Surface Reflectance 8-Day L3 Global 500 m (MOD09A1) product was used. For each pixel, the best observation value in the 8-day record is selected based on high observation coverage, low view angle, absence of clouds or cloud shadow, and aerosol loading.

The key satellite imageries to be used in rice mapping are those taken during the rice-planting calendar. For the delta region in Egypt, the rice-planting season is from mid-April to late October. Each image is to be examined visually and quality flags are checked for clouds or any other inaccuracies. Each image is then clipped to the region to be mapped. For each image, the indices EVI, LSWI, and NDVI are calculated. And rice detection is signaled if the condition LSWI > EVI or LSWI > NDVI is met.

Figs 3-1 and 3-2show the behavior of LSWI, NDVI, and EVI throughout the rice-planting season. In Fig3-1in a rice field the LSWI exceeds EVI in the image dated 18/6 signaling transplanting of rice. In Fig3-2 in a different rice field the LSWI does not exceed EVI or the NDVI throughout the planting season raising the need to modify rice detection criteria.Fig 3-3 shows the difference between the EVI and LSWI for the same rice field in Fig 3-1. From Fig 3-3 the min value of EVI-LSWI occurs in 18/6 with a value of -0.05 signaling transplanting of rice. The difference between EVI and LSWI for the rice field of Fig 3-2 is shown in Fig 3-4 where a negative value does not occur instead the min value is 0.02 between EVI and LSWI for the whole rice-planting period.

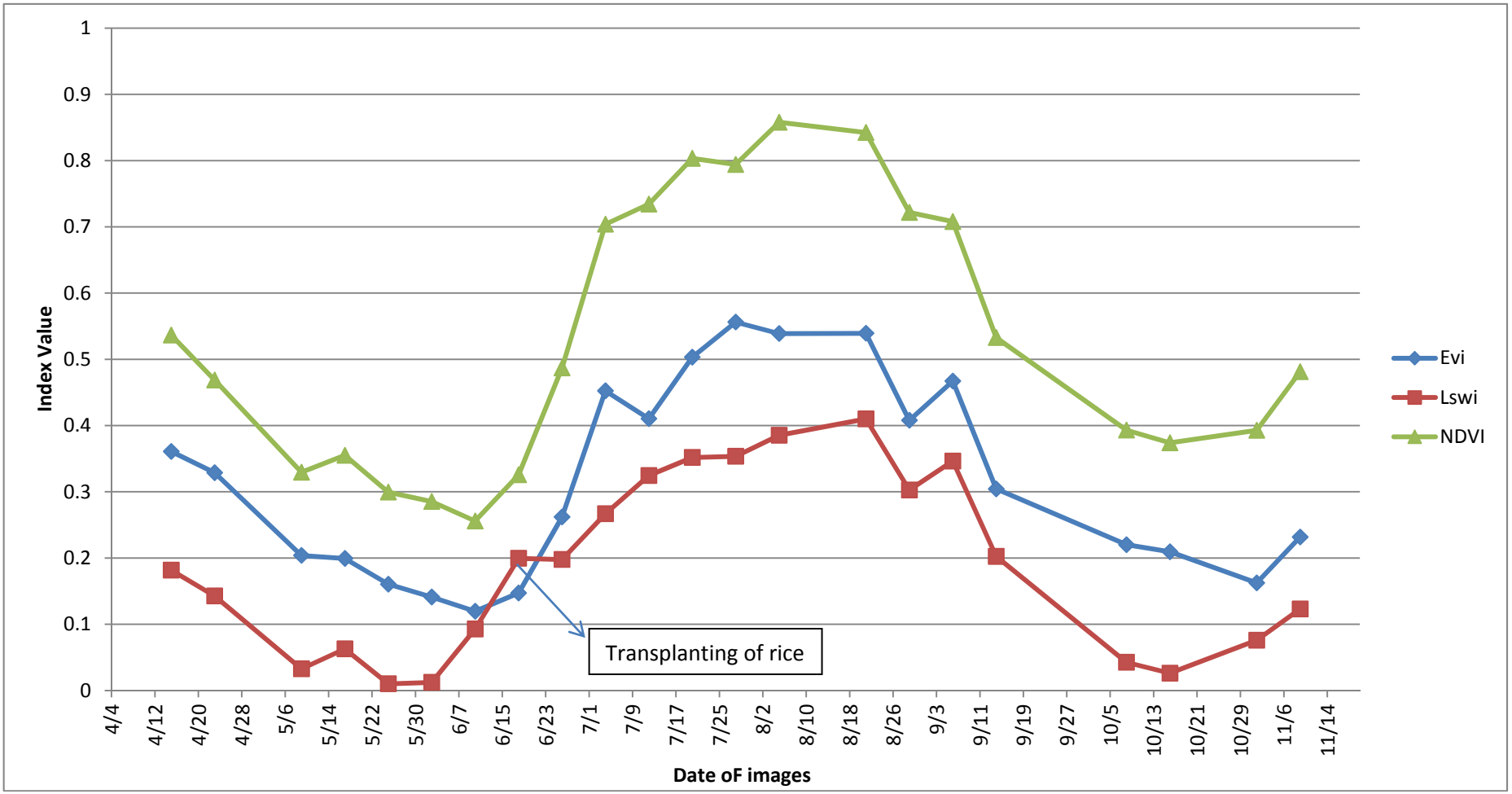


Fig 3-1: LSWI, NDVI and EVI indices for a rice field during the planting season

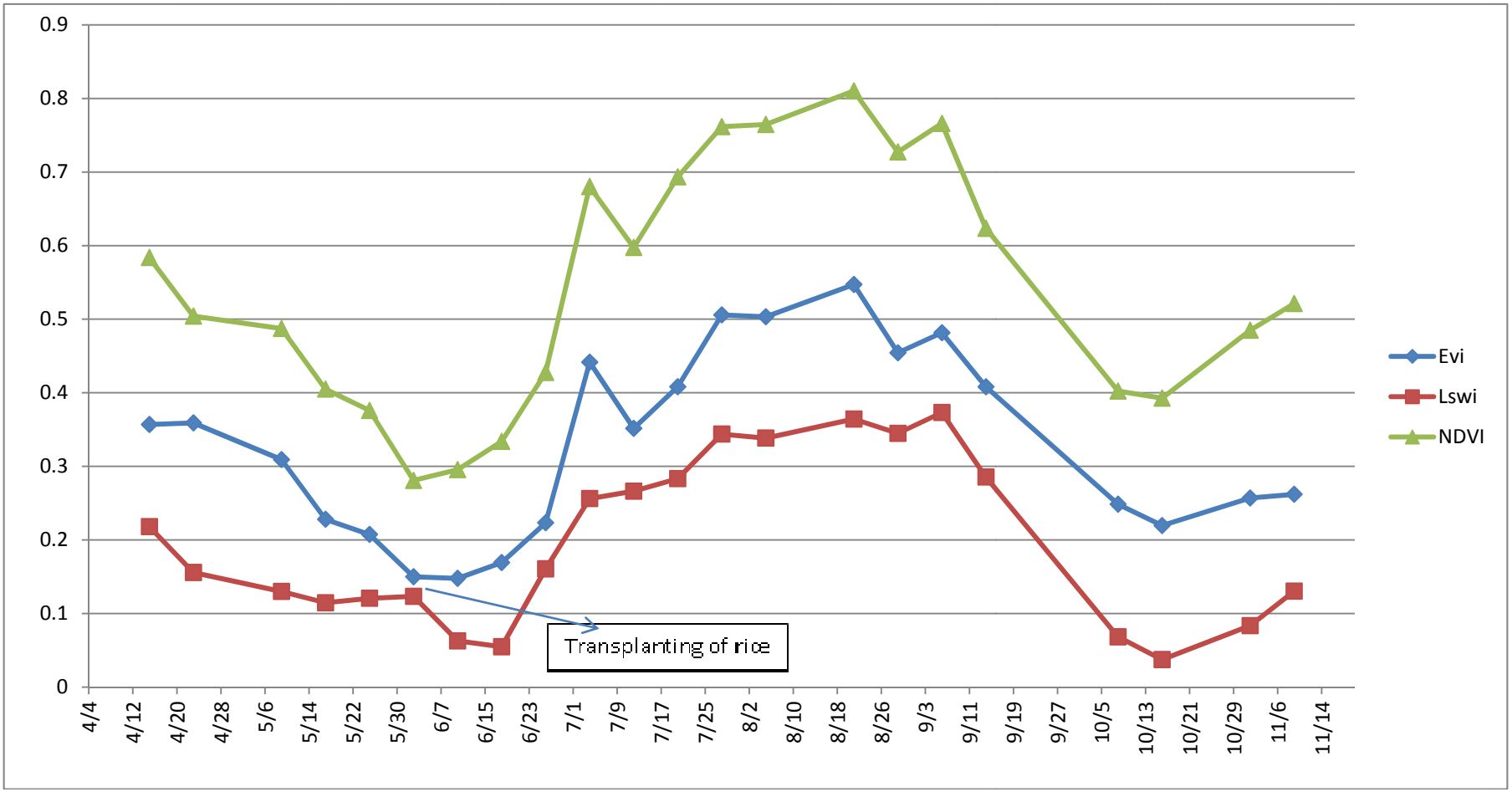


Fig 3-2: LSWI, NDVI and EVI indices for a different rice field during the planting season

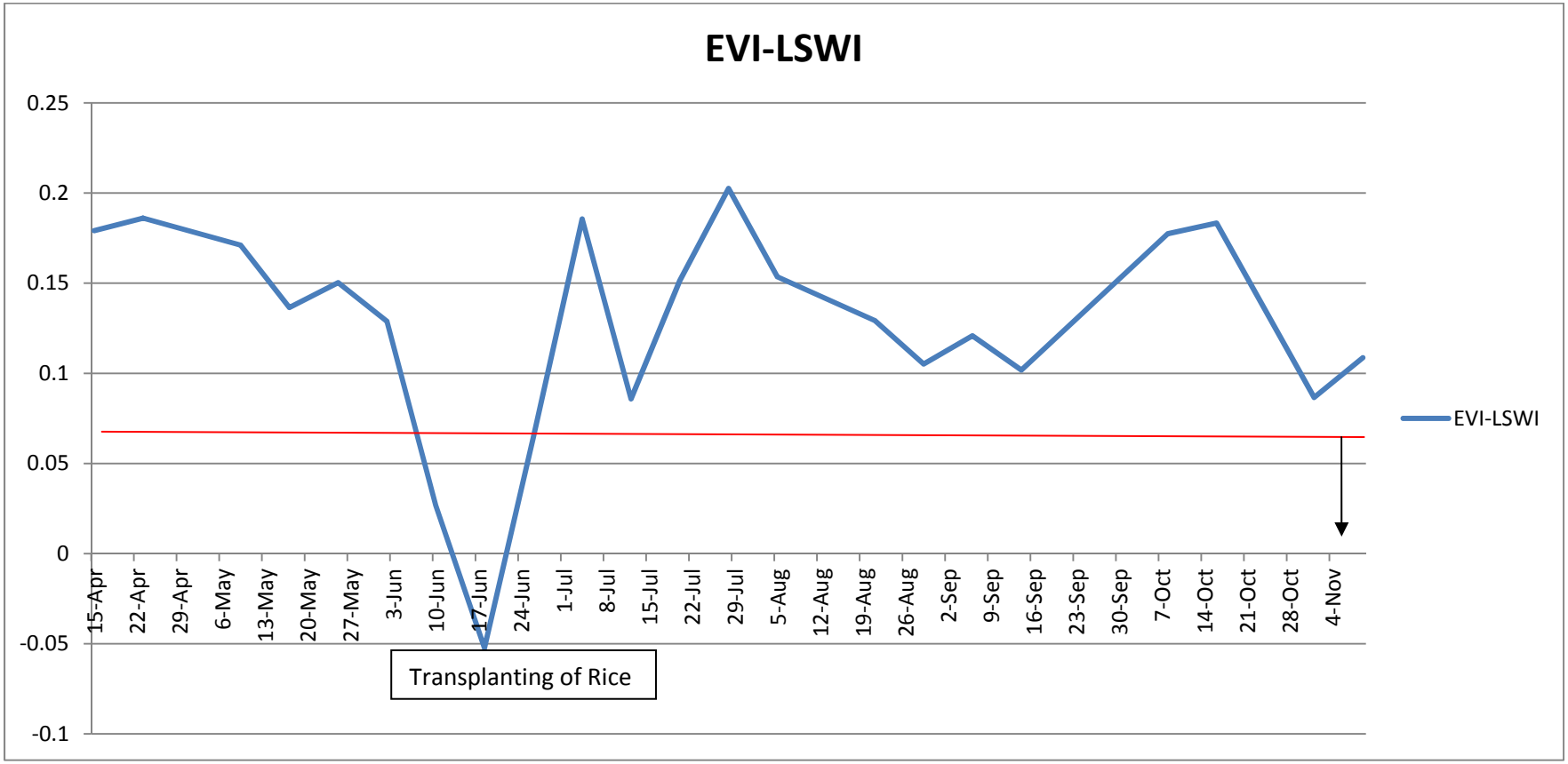


Fig 3-3: Difference between EVI and LSWI for the rice field of Fig 3-1during the planting season

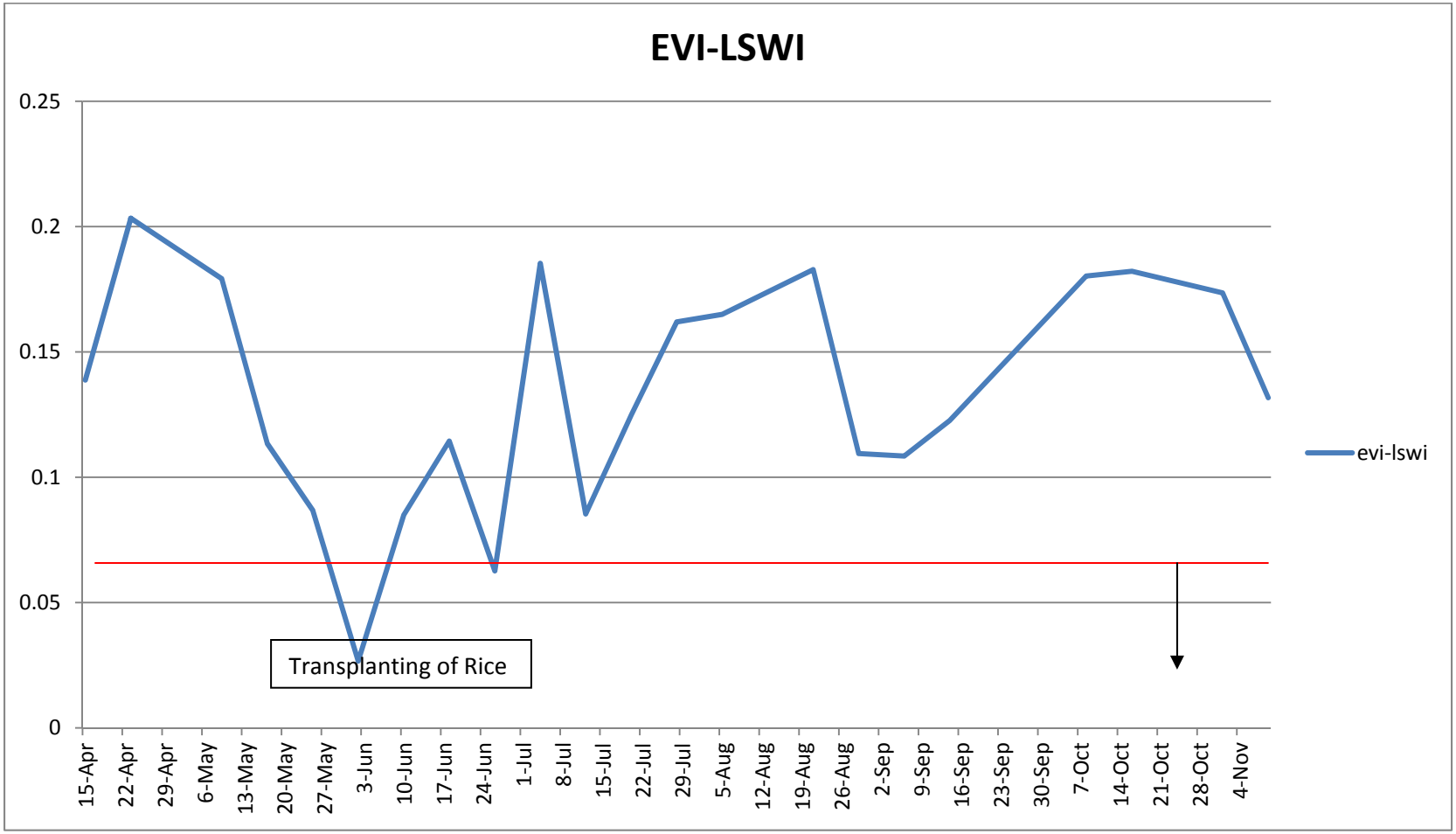


Fig 3-4: Difference between EVI and LSWI for the rice field of Fig 3-2 during the planting season

### 3.1.1 Cloud Contamination Correction

Although MOD09A1 records pixels with low cloud coverage, there are still pixels contaminated with clouds. These pixels could be misclassified as rice. This is because it will have a LSWI greater than EVI or NDVI. In order to mitigate this misclassification potential, a model was built to check for clouds. Clouds reflectance in the blue band is typically greater than 0.2 thus a simple condition of testing the blue band reflectance was used to mask the cloudy pixels (Blue reflectance > 0.2 therefore clouds).

### 3.1.2 Permanent Water and Fish Farms Correction

Following the rice mapping assumption, permanent water bodies or fish farms may be classified as rice. In order to avoid this misclassification potential the permanent lakes and water bodies are masked from the MODIS imagery by their shape files. In addition, if a pixel satisfies the criteria of LSWI + $\Delta$ > NDVI or LSWI + $\Delta$> EVI in more than 6 dates this signals that this pixel is not rice but rather water. In a rice field the vegetation cover starts to grow and will cover the water in the field in nearly forty day duration of the planting season.

### 3.1.3 Rice Planting Calendar Correction

Another condition is applied if the date of satisfying the rice planting detection criteria takes place after end of August then the pixel will be classified as water as this is not possible according to the rice-planting calendar.

### 3.1.4 Relaxation Factor Determination ($\Delta$-parameter)

As it was shown from Fig 3-2, the LSWI does not exceed the EVI or the NDVI although field survey indicated the presences of rice fields in this pixel. Instead, the LSWI approach the value of EVI in the image dated 2/6 but does not cross it as per the

previously mentioned criteria. One reason for this case could be related to averaging, i.e. the majority of the pixel is rice, but not its entirety. Therefore, a modified criterion for detecting rice planting is needed. From the literature the relaxation assumption used is 0.05 (Xiao, 2002; Sun, 2009; Xiao, 2005; Xiao, 2006).

The modified criteria adopted will be LSWI + Δ > EVI or LSWI + Δ > NDVI will signal rice transplanting. The Δ-parameter will be obtained as best fit of each rice-growing region.

### 3.1.5 Rice area tuning

The drawback of the MODIS imagery is its coarse resolution. In order to refine the rice area detected by MODIS imagery, the rice-mapping algorithm combines mapping of other land covers obtained by higher resolution satellite. For example, LANDSAT TM imagery with 30m spatial resolution if available in earlier years can be used to differentiate between vegetation and non-vegetation areas.

### 3.1.6 Vegetation versus non-vegetation areas mapping Module

The pattern of reflectance differs from vegetation, water and bare soil. The different response pattern can be used for classification. Fig 3-5 shows the spectral response pattern taken for some different class types on a LANDSAT 5 Tm image. Where the x-axis is the wavelength and the Y-axis is the apparent reflectance

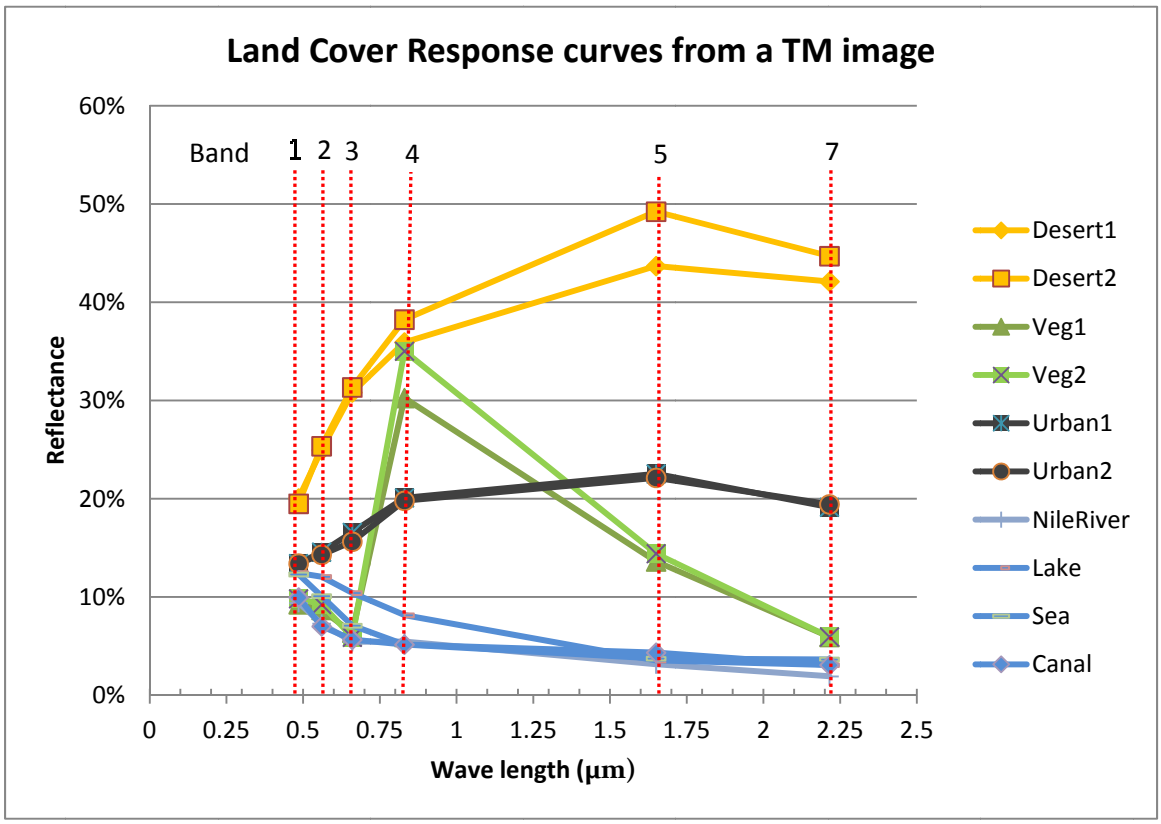


Fig 3-5: Spectral response pattern for some different class types on a LANDSAT 5 Tm image

It can be seen that the vegetation response (the Green Curve in Fig 3-5) is different from that of urban, dessert or water. By examining the spectral response pattern of vegetation, urban, desert, and water which constitute the main land covers in Egypt it can be seen that both vegetation and water have a smaller reflectance in the mid-infra wavelength MIR (band 5) compared to near Infra-red wave length NIR( band 4). On the

other hand, urban (or bare Soil) and Desert features have a greater reflectance in the mid-infrared wavelength (band 5) compared to near Infrared wavelength (band 4). Defining an index and naming it Index1 Eq 3-1 containing both NIR and MIR and making use of this phenomenon we can differentiate water and vegetation areas from urban and desert. This index is calculated by Eq 3.1, and will have a negative value for vegetation or water. The second step is to differentiate between water and vegetation by making use of the normalized difference vegetation index NDVI that relates between the reflectance in the red and NIR wavelengths. For water, this index will be negative or will reach a 0.1 threshold as water reflects less in the NIR than in the red wavelength on the other hand vegetation has a higher reflectance in the NIR portion than that in the red region.

**Index 1 = (MIR- NIR) / (MIR+NIR)** **Eq 3-1**

Where

MIR is mid infrared reflectance

NIR is near infrared reflectance

To differentiate between urban and desert classes the spectral response pattern shows that, the desert has a greater reflectance in band seven than that of urban. Trying to find the threshold that can distinguish between desert and urban many pixels in desert and urban classes were examined. It was found that the reflectance in band seven in urban areas would be less than 0.3, which will be used as a threshold to distinguish between urban and desert classes. The module can be applied using any satellite image containing the following bands (Red, NIR, MIR).

Fig 3.6 shows a flowchart summarizing the steps carried out by the mapping module to differentiate among the four key land covers: water, vegetation, desert and urban areas. For this classification, high or medium resolution imageries can be used even if their date is not in the rice-plantation period or even the same year when rice mapping is carried out.

Fig 3-6:Flowchart showing vegetation versus non-vegetation areas mapping module.

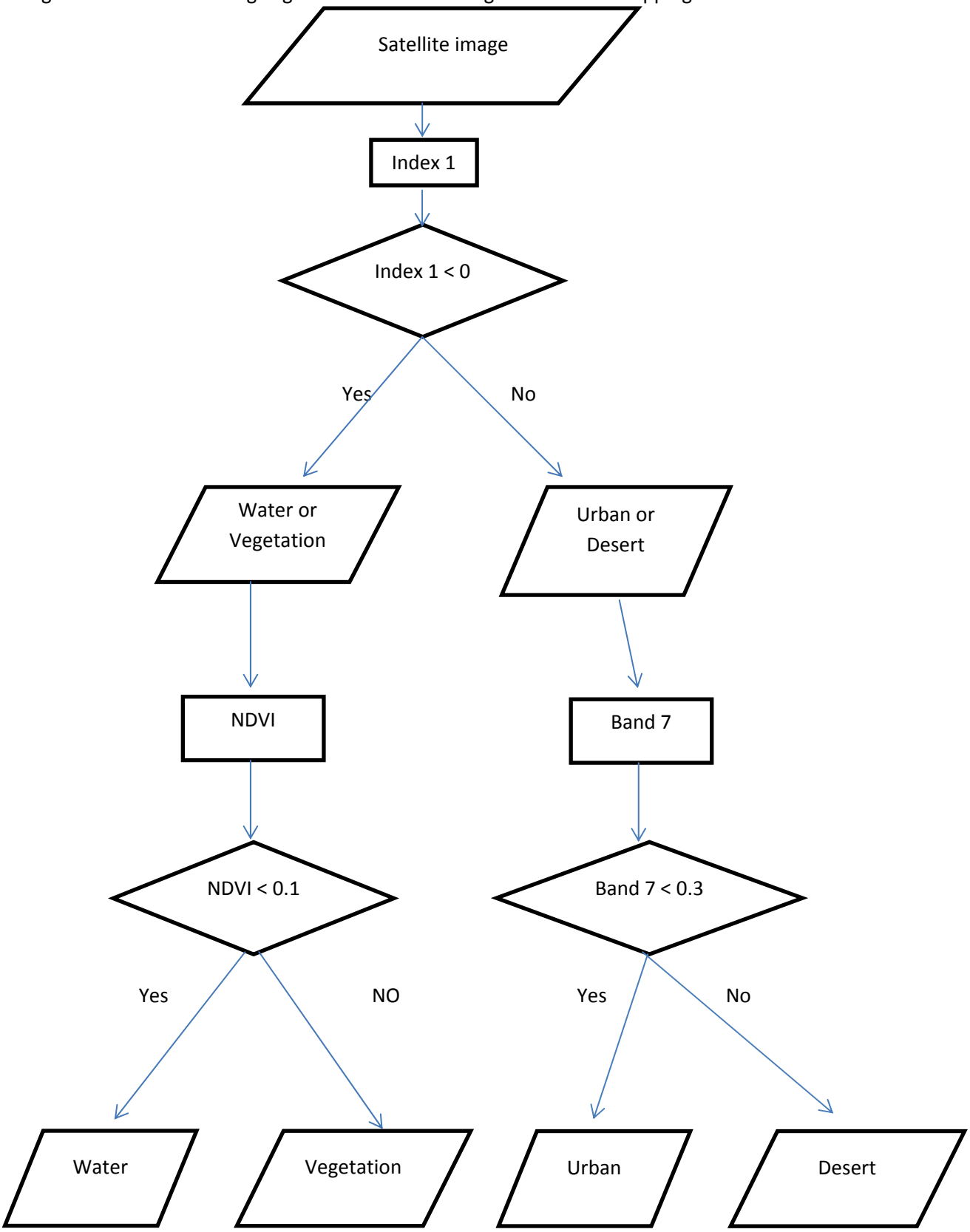

The results from applying this algorithm are then used to refine the rice area mapping from the MODIS imagery. Thus the rice mapping algorithm can be summarized in the following steps and flowchart.

### 3.2 Steps of the rice Mapping Algorithm

The steps of the rice mapping algorithms can be summarized as follows

1- Download the MODIS satellite images MOD09A1 MODIS Terra/Aqua Surface Reflectance 8-Day L3 Global 500 m ( or an equivalent free satellite image for the rice plantation period with highest available resolution)
2- If the terra images are not available due to clouds or any other reasons we may use the Aqua images
3- Check for clouds and hazy areas through visual interpretation and examining the quality flags in the MODIS image
4- Use a module in the algorithm to use the available information in terra or aqua by replacing the cloudy pixels with the clear ones (if available).
5- Clip the MODIS image to the required region to be mapped
6- Mask the area of lakes and desert from the image by a digitized shape file or it can be masked from the refinement module.
7- Reproject the image to the UTM projection

8- Calculate EVI for the masked images during the plantation period as follows
   **EVI = 2.5*(NIR - RED/ (NIR + 6 * RED -7.5* BLUE + 10000))**
   Where

   NIR = the near infra-red band (841-876 nm)
   Red=the red band (620-670 nm)
   Blue= the blue band(459-479 nm)

9- Calculate the LSWI for the masked images during the plantation periodas follows
   **LSWI = (NIR- SWIR) / (NIR+ SWIR)**
   Where

NIR = the near infra-red band (841-876 nm)

SWIR=the short wave infra-red band (1628-1652 nm)

10- Calculate the NDVI for the masked images during the plantation periodas follows

**NDVI= (NIR – RED) / (NIR + RED)**

Where

NIR = the near infra-red band (841-876 nm)

Red=the red band (620-670 nm)

11- Tune the files by subtracting the non-vegetation area ( urban and desert) obtained from the vegetation versus non vegetationareas mapping algorithm

12- Run the model for rice detection using the modified criteria

LSWI + Δ > EVI or

LSWI + Δ > NDVI

If the above condition is met then rice pixel is signaled

13- Identify the water bodies by checking if the rice pixel is signaled in more than six images or after the end of August and delete it from the classified rice pixels

14- Find the rice area transplanted in each date

15- Clip by the admin boundaries and find the rice transplanted in each date

The rice mapping algorithm flowchart is presented in Figure 3.7

Fig 3-7: Flowchart showing Rice areas Mapping algorithm

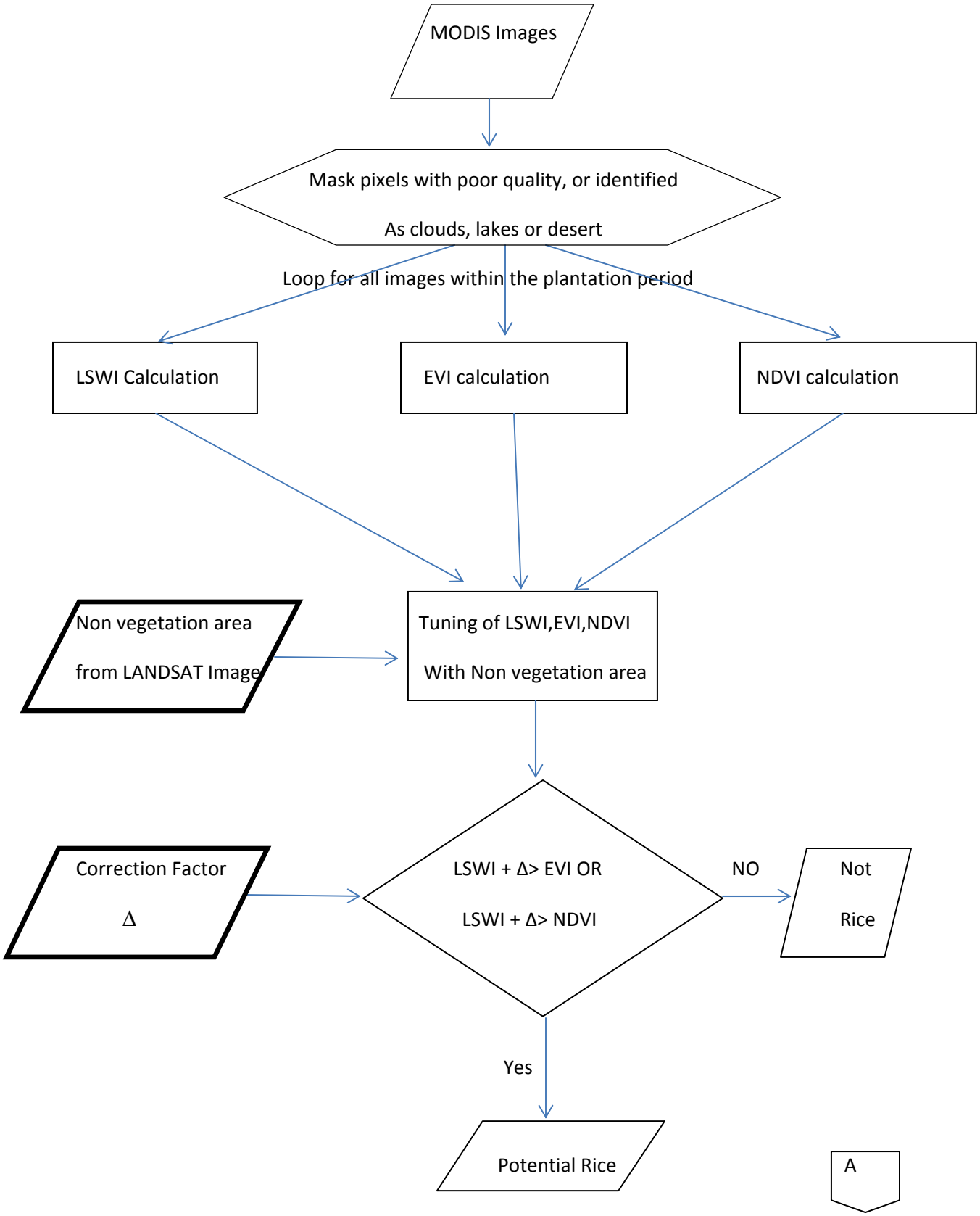

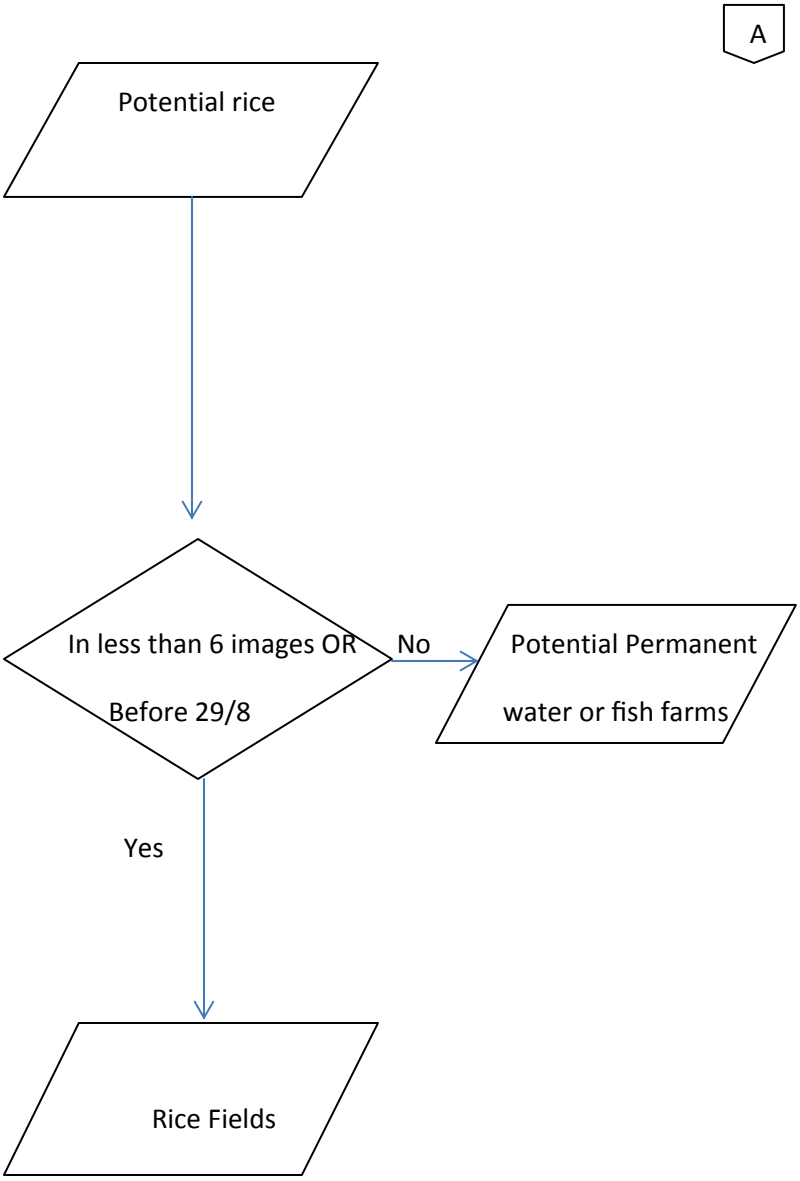
A
Potential rice
In less than 6 images OR
Before 29/8
No
Potential Permanent
water or fish farms
Yes
Rice Fields

# Chapter 4

# The Application of the Rice Mapping Algorithm on the Delta region of Egypt

## 4.1 Study Area:

Rice is mainly planted in Egypt delta region. The delta area is about 30,000 $km^2$. The delta region is bounded in the north with the Mediterranean Sea, in the west with the western desert, in the east with the eastern desert and in the south with the Egyptian capital Cairo. It covers the area south-north from 30˚ 4’ N to 31˚ 36’ N and east-west from 32˚ 12’ E to 29˚ 25’ E. The main governorates in planting rice are Daqhliya, Kafrelsheikh, Sharqeya, Beherah, Gharbeya and Dumyat. The boundaries of each governorate are shown in Fig 4-1.

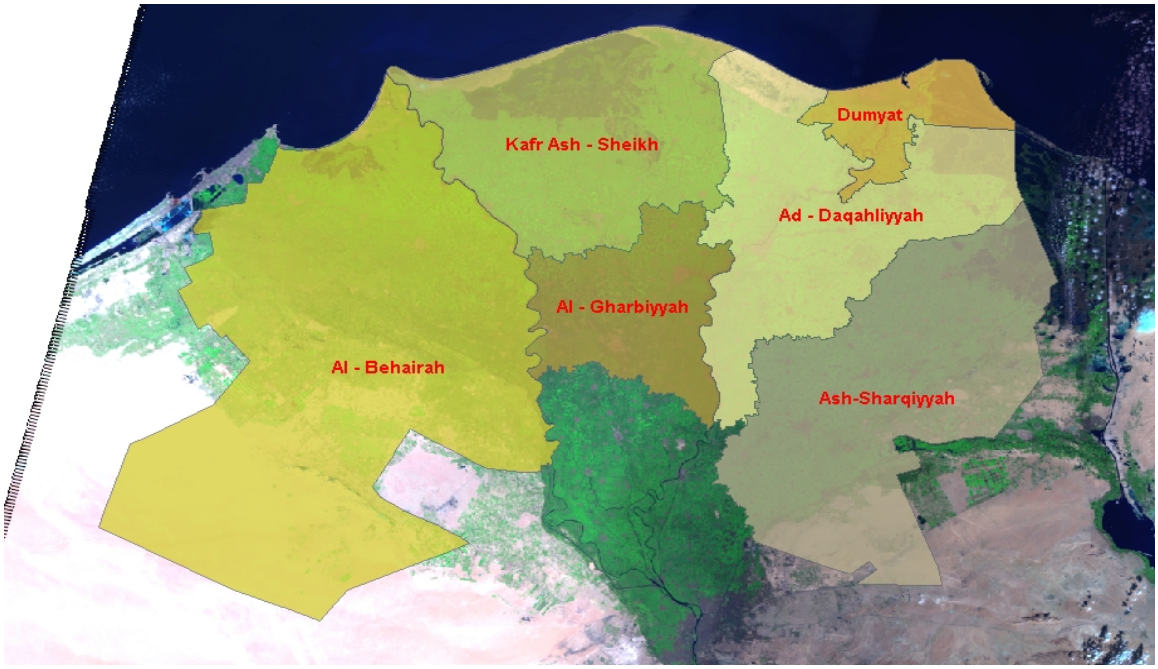


Fig 4-1: Delta region and Rice planting governorates

### 4.2 The Application of Vegetation versus Non-vegetation Areas Mapping Module

The satellite images used were LANDSATTM images. The thematic Mapper TM satellite bands characteristics as described by the United States geological survey USGS is summarized in Table 4.1.

Table 4-1: LANDSAT TM Bands

| Thematic Mapper (TM) | LANDSAT 4-5 | Wavelength (micrometers) | Resolution (meters) |
|---|---|---|---|
| | Band 1 | 0.45-0.52 | 30 |
| | Band 2 | 0.52-0.60 | 30 |
| | Band 3 | 0.63-0.69 | 30 |
| | Band 4 | 0.76-0.90 | 30 |
| | Band 5 | 1.55-1.75 | 30 |
| | Band 6 | 10.40-12.50 | 120* (30) |
| | Band 7 | 2.08-2.35 | 30 |

Two shifted LANDSAT TM scenes can cover the delta region in Egypt. This is shown in Fig 4-2. In the mid and east delta part, a shifted scene combined of scenes 176/

38 and 39 is used. In the western delta part a shifted scene combined of scenes 177/ 38 and 39 is used. To enhance the delineation accuracy of non-vegetation areas, the algorithm was applied on both summer and winter season images in each region. If the pixel is classified as non-vegetation (Urban or Desert) in both summer and winter image it is considered as non-vegetation. Table 4-2 summarizes the images used. Fig 4-2 shows the layout of the scenes covering the delta region and the LANDSAT TM images path and row numbers.

Table 4-2: Summary of the images used

| | Mid and Eastern Delta | Western Delta |
|---|---|---|
| LANDSAT 5 Tm Scene path and row | 176 / 38 and 39 | 177 / 38 and 39 |
| Dates | Summer Image 5/6/2009<br>Winter Image 13/2/2009 | Summer Image 12/6/2009 |
| Bands used | Band 3, Band4, Band 5 | Band 3, Band 4, Band 5 |
| Scene coverage area | ~ 170 km north-south by 185 km east-west | ~ 170 km north-south by 185 km east-west |

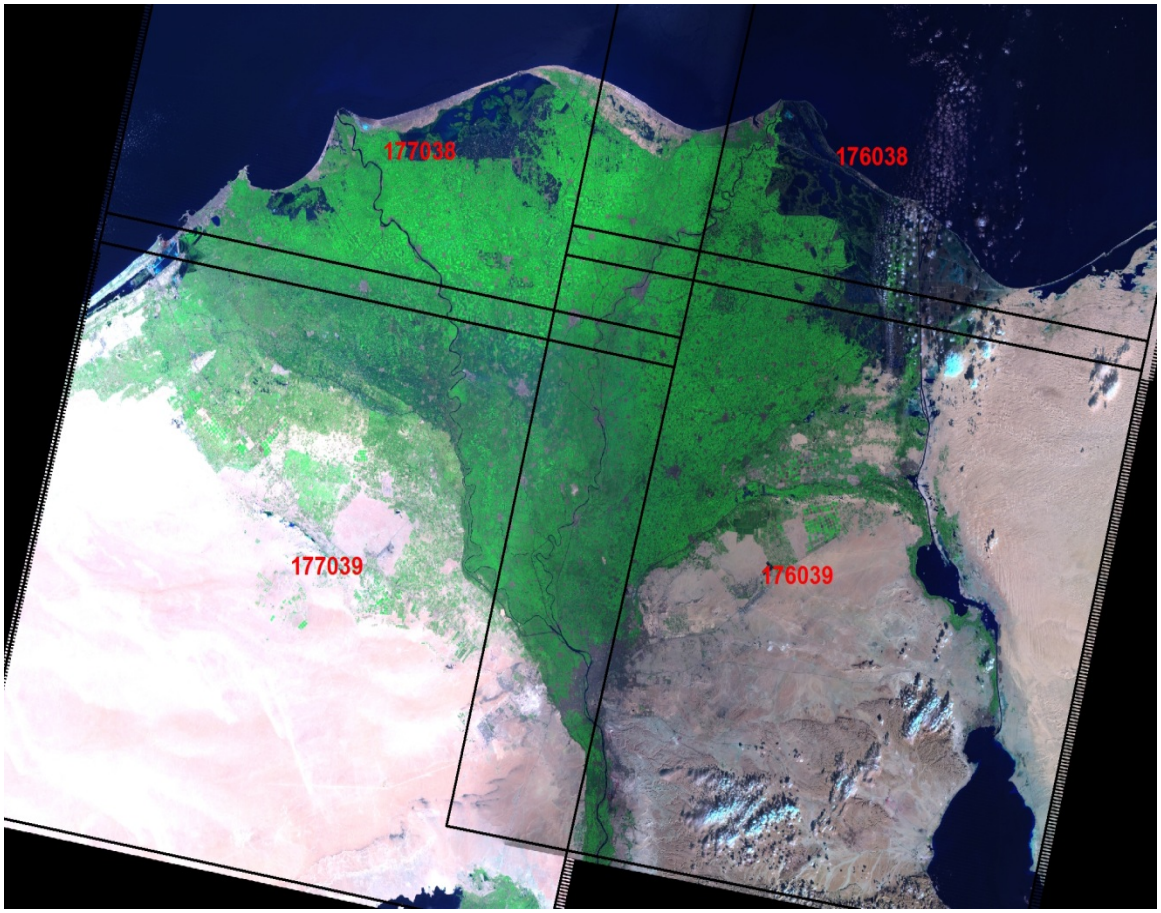


Fig 4-2: Delta LANDSAT 5 Tm Mosaic (Year 2005) showing scenes path and row number

These images were used to classify land covers (vegetation versus non-vegetation) in the various governorates of the delta region of Egypt following the procedure outlined in Figure 3-6. Table 4-3 summarizes the results of land classification in the East delta governorates while middle and west delta governorates classification results are shown in Table 4.4

Table 4-3:East Delta Governorates land classification

| | Sharqeya | Ismailiya | Suez | Pursaed | Dumyat | Daq | Qalyoubeya |
|---|---|---|---|---|---|---|---|
| Veg(Feddan)rounded | 903200 | 256200 | 33600 | 121900 | 135600 | 805300 | 206800 |
| Urban(Feddan)rounded | 55600 | 38200 | 14600 | 87300 | 16700 | 48800 | 25100 |
| Desert(Feddan)rounded | 169000 | 798600 | 690500 | 7800 | 400 | 5800 | 32800 |

Table 4-4:Middle and West Delta Governorates land classification

| | Menofeya | Gharbeya | Kafrelsheikh | Alex | Beherah |
|---|---|---|---|---|---|
| Veg(Feddan) Rounded | 384200 | 364100 | 548400 | 112800 | 1107800 |
| Urban(Feddan) Rounded | 66100 | 85600 | 100700 | 74500 | 328600 |
| Desert(feddan) Rounded | 124300 | 200 | 3400 | 226300 | 836100 |

Fig 4.1 maps the land classification in the delta region of Egypt (vegetation, urban and desert areas). Figures 4.2 and 4.3 are bar chart plots of the land classification given in Tables 4.3 and 4.4. This classification is consistent with the land classification maps of the region.

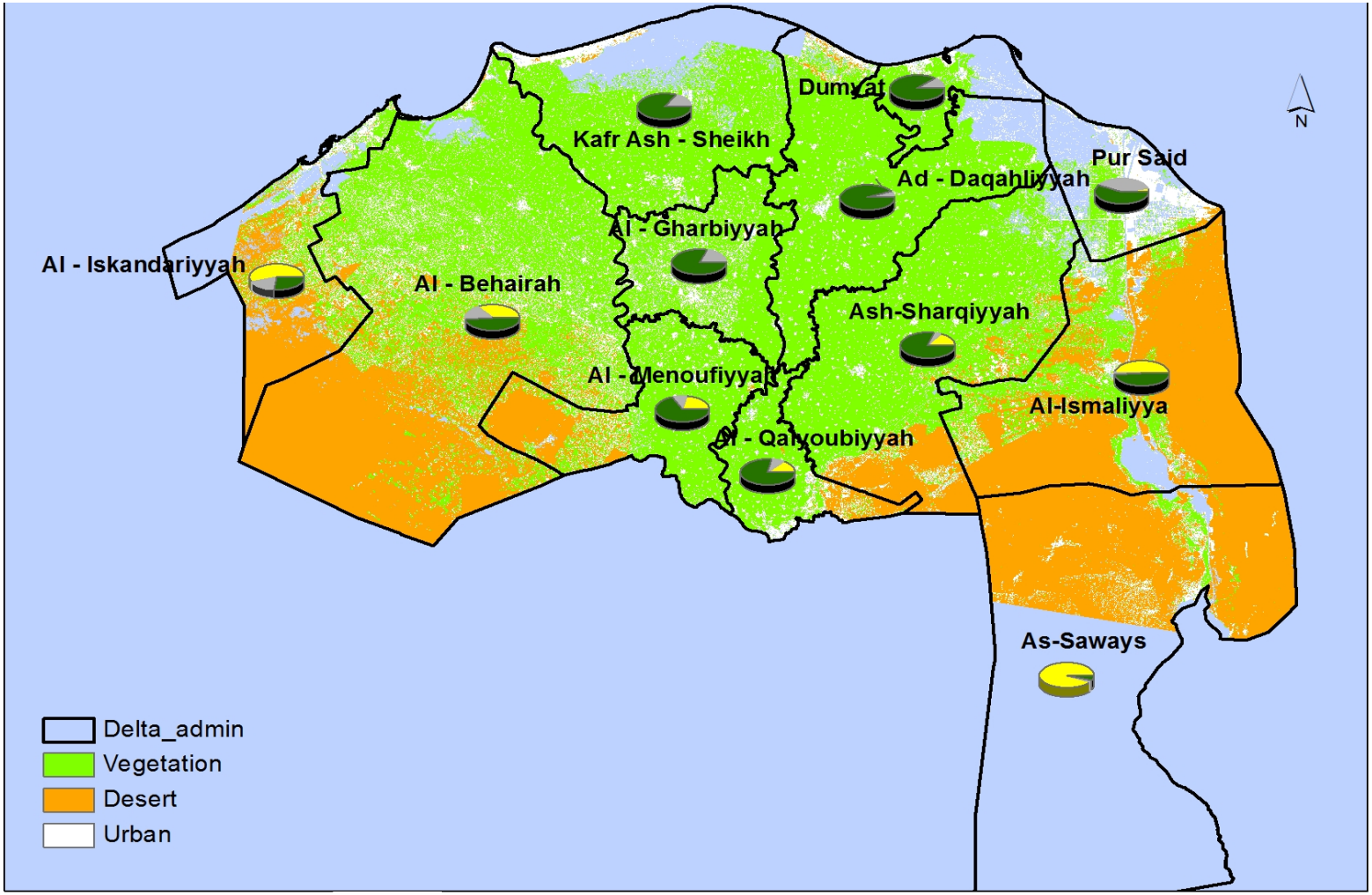


Fig 4.3: Algorithm output of vegetation, desert and urban areas of the delta region of Egypt

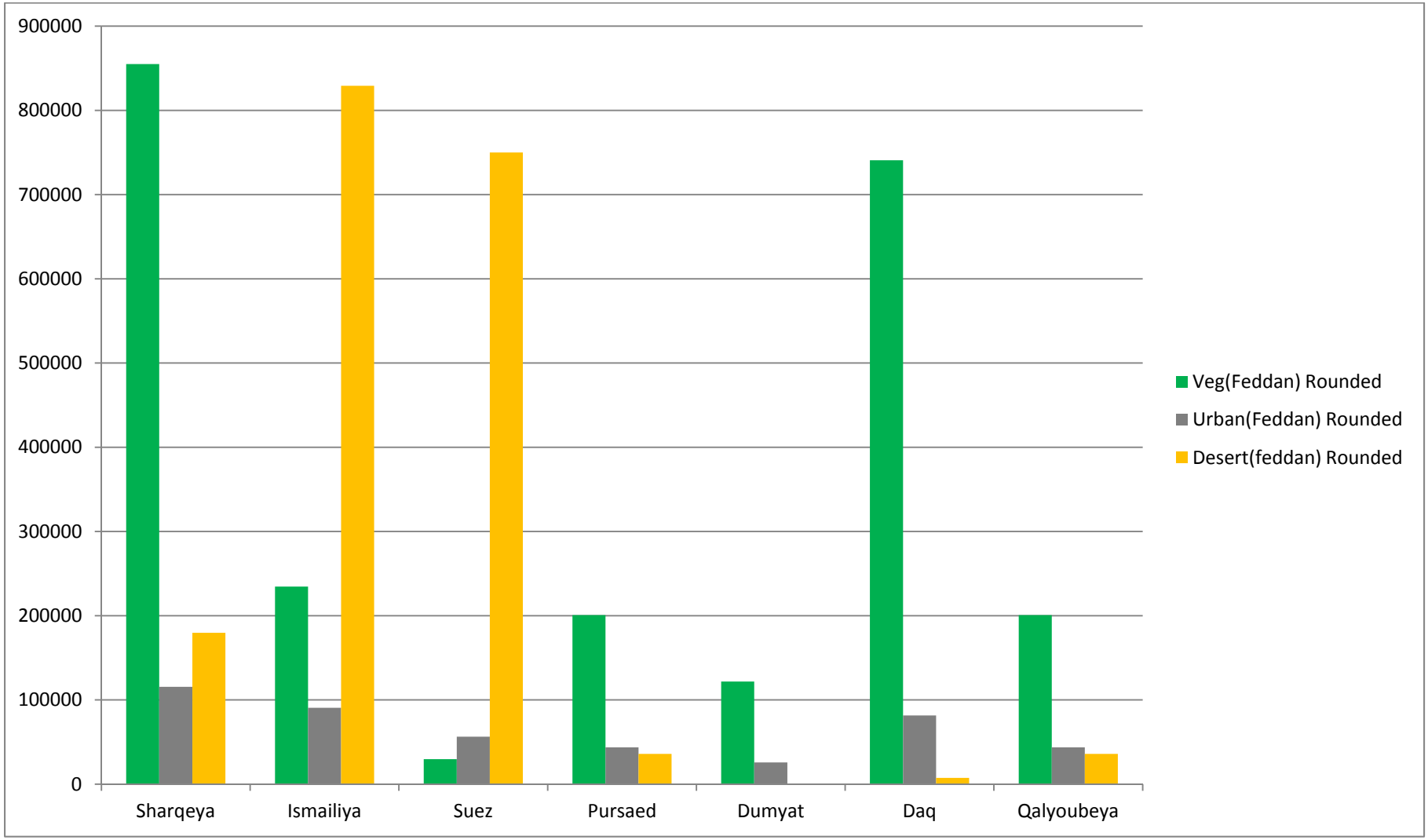


Fig 4-4: East Delta Governorates Categories

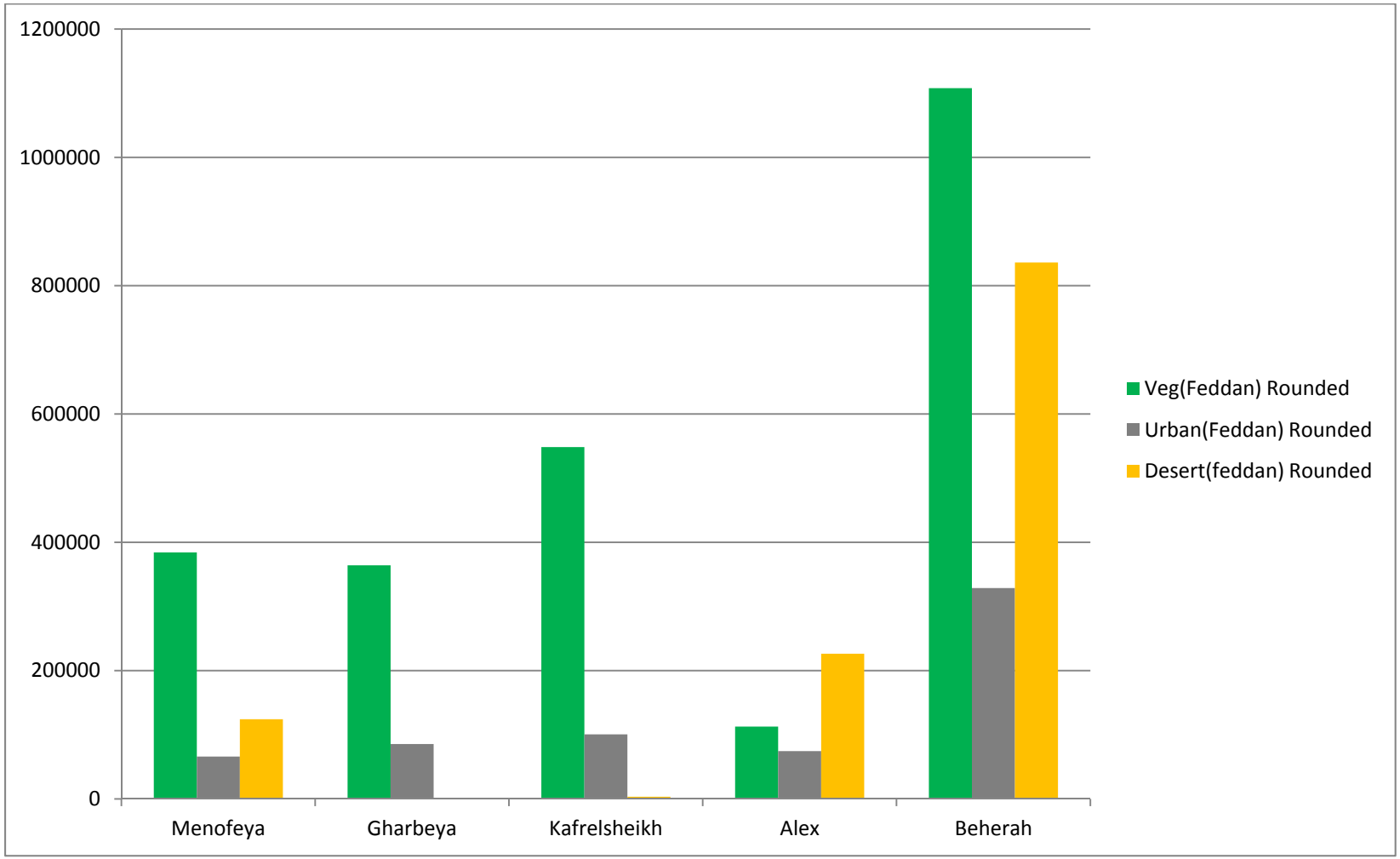


Fig 4-5: Middle and West Delta Governorates Categories

## 4.3 The Analysis of LSWI, NDVI, and EVI Dynamics for Rice Mapping

### 4.3.1 Data and Methods

The imagery used for LSWI, NDVI and EVI dynamics analysis were the MODIS Terra/Aqua Surface Reflectance 8-Day L3 Global 500 m (MOD09A1) product. The tile of this product that covers the delta region is h20v5. The MOD09A1 images covering the delta region were downloaded from http://reverb.echo.nasa.gov/reverb/. By examining the rice planting calendar in Egypt the imagery from 15-April till 9- November 2009 were obtained.The delta region area of interest was used to clip the images. Each image is then projected to the UTM zone 36 with the WGS84 datum to have the same projection with the available main lakes and desert areas, Nile River, and governorates boundaries GIS shape files. The shape files were superimposed on the MODIS imagery to mask their areas out. These images were utilized for rice mapping by analyzing the LSWI, NDVI, EVI dynamics in the various governorates of the delta region of Egypt following the procedure outlined in Figure 3-7.

### 4.3.2 Calibration of the Δ-parameter

As stated in section 3.2.4 the modified criteria used to signal rice transplanting is LSWI + Δ> EVI or LSWI + Δ> NDVI. In order to obtain the Δ-parameter as best fit of each rice-growing region, known rice fields that were collected in 2009 and 2010 were used to examine the relation of LSWI, EVI and NDVI throughout the planting season in these fields. The samples collected covers about 325 Km2 (77450 feddans) in 2009 and 384 $km^2$ (91500 feddans) in 2010. They are distributed among the following governorates Behera, KafrElsheikh, Daqheliya, Dumyat, Sharqeya and Gharbeya which represents the highest 6 governorates in rice planting in Egypt (Ministry of agriculture reports).

Although rice transplanting occurs on different dates and differs from one region to another, the period chosen to calculate the LSWI,EVI and NDVI covers almost all the transplanting dates' differences. The period was from the beginning of May until the beginning of August. The indices LSWI, EVI, and NDVI were calculated for each rice pixels of the known fields. The difference EVI-LSWI was calculated. The min of EVI-LSWI for every known rice field pixel was recorded. It was found that for every governorate known rice fields this min value can be averaged and presented in Table4-5.

Table 4-5: The ΔEVI-parameter for each governorate

| **Gover(evi-lswi)** | **2010** | **2009** |
|---|---|---|
| | Mean | |
| KafrElsheikh | 0.044 | 0.042 |
| Dumyat | 0.042 | 0.034 |
| Sharqeya | 0.053 | 0.05 |
| Gharbeya | 0.05 | 0.054 |
| Behera | 0.072 | 0.073 |
| Daqhleya | 0.045 | 0.057 |

For each governorate, the corresponding ΔEVI-parameter is used in the rice-mapping algorithm. For governorates Kafrelsheikh and Dumyat the Δ-parameter is 0.04. For governorates Daqehleya, Gharbeya and Sharqeya the Δ-parameter is 0.05. For Behera governorate the Δ-parameter is 0.07.

Applying the same steps as for EVI, the difference NDVI-LSWI was calculated. The min of NDVI-LSWI for every known rice field pixel was recorded. It was found that for every governorate known rice fields this min value can be averaged and presented in Table 4-6.

Table 4-6: The ΔNDVI-parameter for each governorate

| **Gover(ndvi-lswi)** | **2010** | **2009** |
|---|---|---|
| | Mean | |
| KafrElsheikh | 0.184 | 0.164 |
| Dumyat | 0.177 | 0.18 |
| Sharqeya | 0.172 | 0.187 |
| Gharbeya | 0.197 | 0.198 |
| Behera | 0.23 | 0.233 |
| Daqhleya | 0.155 | 0.154 |

It was found that the Δ-parameter is different if the EVI or the NDVI are used. The Δndvi parameter for KafrElsheikh was 0.174, for Dumyat was 0.178, for Sharqeya was 0.18, for Gharbeya was 0.197, for Behera was 0.23, and for Daqhleya the Δndvi parameter was 0.155. The difference in the Δ-parameter for each governorate may be attributed to rice fields' sizes and its relation to MODIS pixel size, planting practices, orientation of the fields with MODIS pixels, difference between date of fields flooding and image acquisition date.

### 4.4 Validation of Results and Discussion of Vegetation versus Non-vegetation Areas Mapping Module

The land classification obtained by the vegetation versus non-vegetation module of the rice mapping algorithm and presented in map 4.1, was validated according to the scheme outlined in Figure 4-6. 1000 samples of the classification in east delta were randomly selected and validated with very high resolution satellite imagery (60 cm resolution). A 3 * 3 pixel window was used to randomly select equal number of samples for each class category. The results of validation are shown in the confusion matrix of Table 4-7.

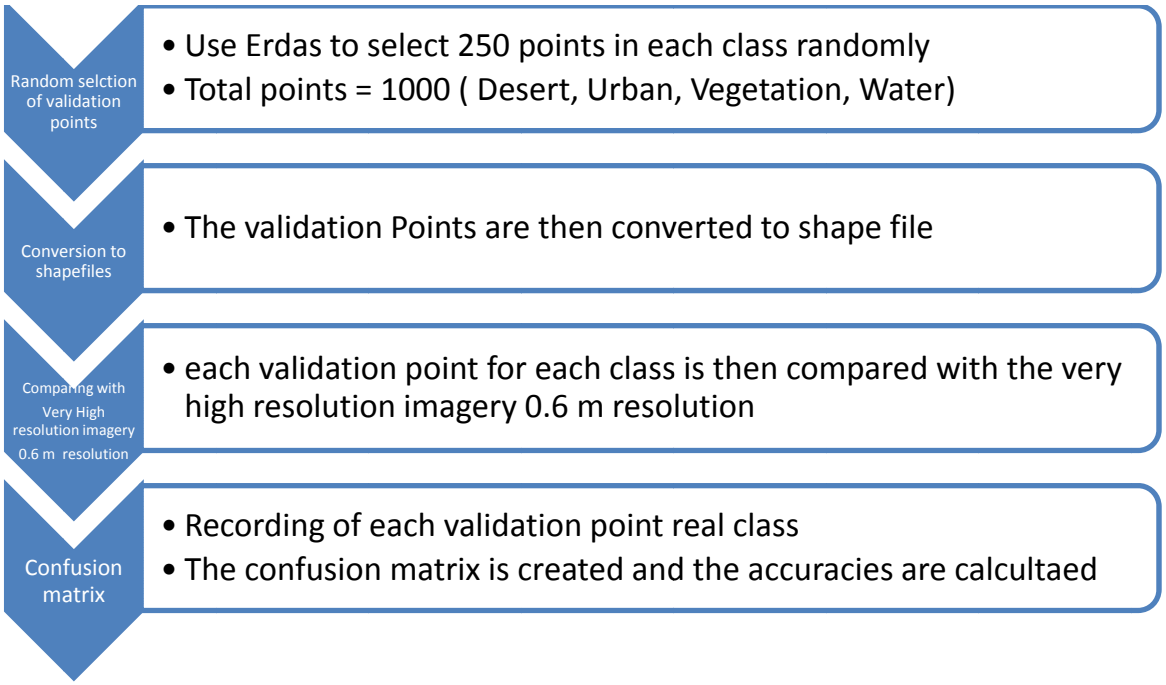


Fig 4-6: Validation procedure for the veg versus non-veg classification module

Table 4-7: Confusion matrix and accuracies

| | Reference samples | | | | | |
|---|---|---|---|---|---|---|
| **Predicted** | | | | | | |
| | **Desert** | **Urban** | **Vegetation** | **Water** | User Accuracy | Accuracy |
| **Desert** | 231 | 5 | 14 | 0 | 231/250 | 92.4% |
| **Urban or bare land** | 1 | 209 | 27 | 13 | 209/250 | 83.6% |
| **Vegetation** | 3 | 11 | 222 | 14 | 222/250 | 88.8% |
| **Water** | 0 | 4 | 2 | 244 | 244/250 | 97.6% |
| Total | 235 | 229 | 265 | 271 | | |
| Producer Accuracy | 231/235 | 209/229 | 222/265 | 244/271 | | |
| Accuracy | 98.3% | 91.3% | 83.8% | 90% | | |

The overall accuracy equals the correctly predicted classes over the total number of samples (231+209+222+244)/1000 = 90.6 % which is a relatively high classification accuracy (Table 4.7) using the vegetation versus non vegetation mapping module. Table 4.7 shows that for example the classification process accurately classified 244 out of 250 water samples, 222 out 250 vegetation samples, 209 out of 250 urban or bare land samples and 231 out of 250 desert samples. The user accuracy which reflects the probability that a classified land cover is in reality that land cover for the main classes was as follows. The percent accuracy for predicting desert, urban or bare land, vegetation and water were 92.4 %, 83.6 %, 88.8% and 97.6 % respectively.

The producer accuracy, which reflects the probability that a certain land cover in the ground is classified as such,for the classes desert, urban or bare land, vegetation and water were 98.3 %, 91.3 %, 83.8% and 90 % respectively. Actually, the accuracy of the classification itself is much higher as for example the algorithm may result in classifying a pixel as desert although part of it may be new reclaimed area where the vegetation is

sparse. Another source of inaccuracy is the change of the class itself due to time difference between the images. For example, some pixels that were classified as water in the images of 2009 were fish farms that have been filled and vegetated. However, the overall accuracy and classes classification accuracy can be considered very satisfactory.

The results show that the algorithm can be used in obtaining accurately classified classes with no training samples, which saves time, effort and money. The assumed reflectance behaviors of the main class types in each wavelength are efficient in this step of the classification.

## 4.5Application of Rice area tuning from Vegetation versus Non-vegetation Areas Mapping Module

Not only the vegetation versus non-vegetation areas mapping module output shows the class type and location in each governorate but also the results are then used to refine the rice area mapping resulting from MODIS imagery analysis. Table 4-8 presents the results of rice mapping incorporating the vegetation versus non-vegetation module (Tm images) and without its use.

The TM tuning results in a root mean square error = 56000 feddan

Table 4-8: Summary of rice mapping results with and without the veg-non-veg module

| | KafrElsheikh | Behera | Daq | Gharbeya | Sharqeya | Dumyat | Total |
|---|---|---|---|---|---|---|---|
| Without veg-non-veg module | 395400 | 319500 | 536500 | 245700 | 408700 | 57500 | 1963300 |
| With veg-non-veg module | 337500 | 229800 | 472400 | 192600 | 387100 | 51300 | 1670700 |
| % Diff | 17% | 39% | 14% | 28% | 6% | 12% | 18% |

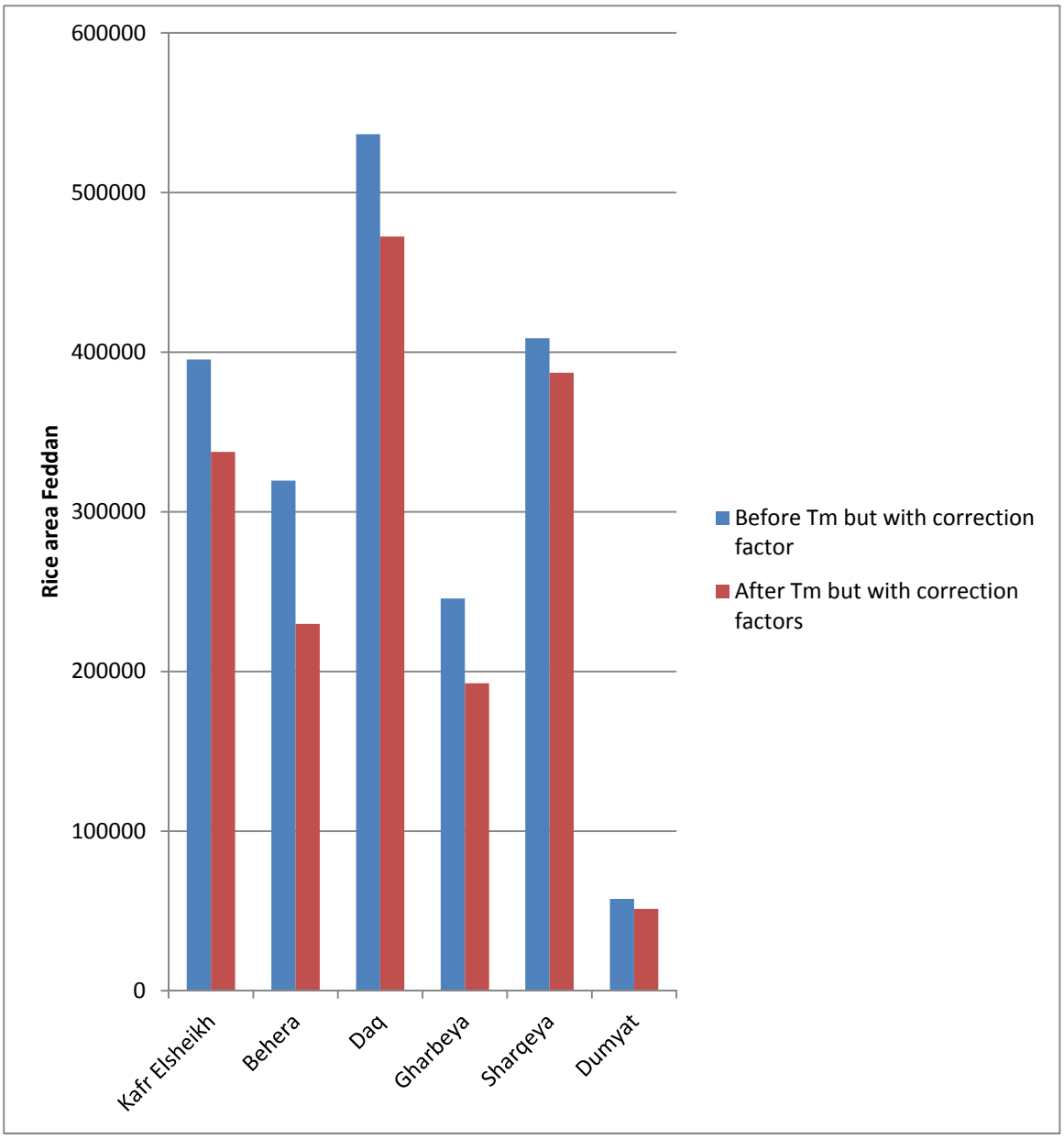


Fig 4-7: Comparison of rice area in each governorate before and after applying veg-non-veg module

It can be seen that using the veg-non-veg module and LANDSAT TM higher resolution image reduced the predicted rice areas in all governorates.

In order to assess the relation between the Δ-parameter and the percentage of MODIS rice area refinement from the application of the vegetation versus non-vegetation module, the percent of refinement against the Δ-parameter was plotted. This is illustrated in Fig 4-8. From Fig 4-8, we can deduce that as the fragmentation increase which is reflected in a more % reduction in MODIS rice area the Δ-parameter increases. The ΔEVI and % reduction in MODIS rice area can be modeled with the second order polynomial equation $y = 0.5598x^2 - 0.1834x + 0.0591$with an $R^2$ equals 0.79. While the ΔNDVI and % reduction in MODIS rice area can be modeled with the second order polynomial equation $y = 0.9852x^2 - 0.27x + 0.1893$ with an $R^2$ equals 0.85.

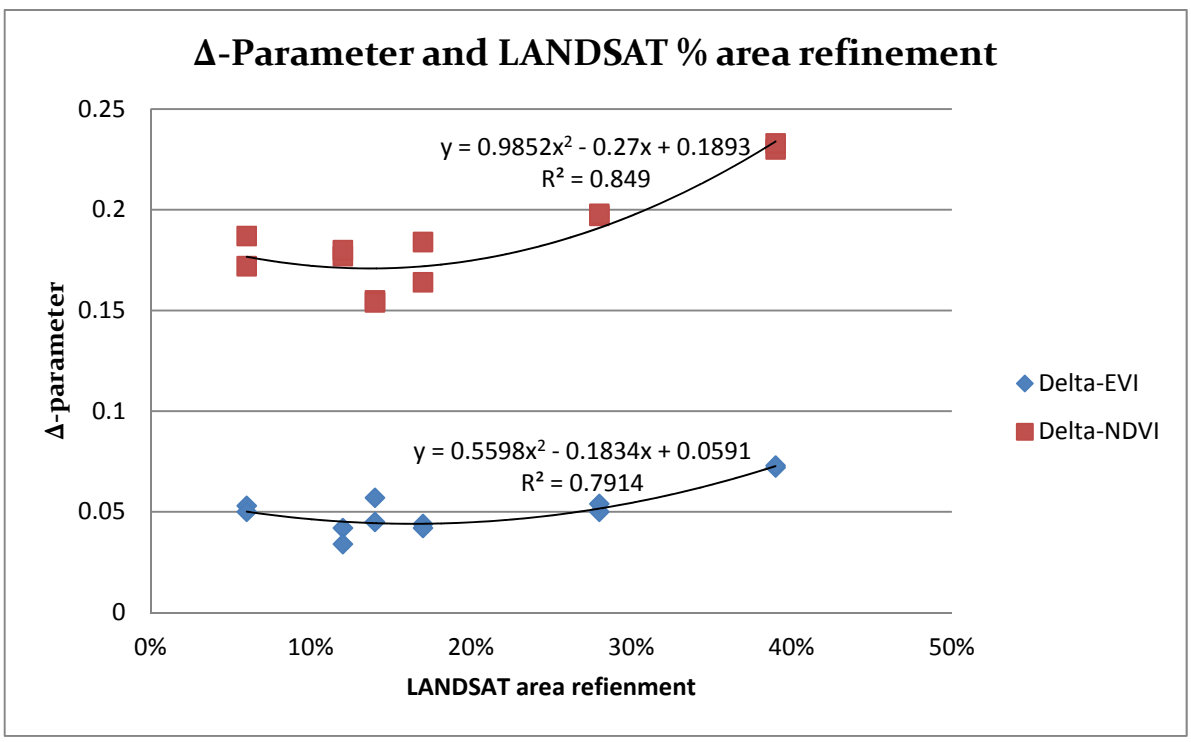


Fig 4-8: Δ-Parameter and LANDSAT % area refinement

### 4.6 Rice Mapping Algorithm Results and Discussion

The rice-mapping algorithm developed is capable of mapping rice areas planted. In addition to identifying the probable rice transplanting date in each pixel classified as a rice pixel.Applying the rice mapping algorithm in year 2009 with the corresponding Δ-parameter and TM tuning for each governorate and for each transplanting date the results are summarized in Table 4-9 and are shown in Fig 4-9.

Table 4-9 shows the rice areas transplanted in each date for each governorate. It can be seen that the max area transplanted occur in the period from 2/6 to 10/6. The transplanting of 1368700 Feddans took place during the period from 17/5 until 4/7; this represents 82% of the total planted rice in 2009. This conforms to local experience within MWRI where the max demand for water due to rice transplanting occurs from end of May until Mid-July. There was no image during the period from 13/8 to 21/8 but during this period a very small area of rice transplanting occurs. In addition, the most critical imagery availability dates in order for the algorithm to well function are from Mid-May until Mid-July.

Fig 4-9 shows the spatial distribution of rice areas and rice transplanting dates in a GIS format. The area of rice transplanted in every governorate geographic location is shown. Moreover, the spatial distribution of the transplanting dates of these areas is revealed.

Fig 4-9 shows that rice transplanting dates in the northern part of the delta are earlier than those of the southern part. In addition, almost no rice is planted in Menoufiya governorate and these findings conform to local experience within MWRI.

Applying the algorithm in year 2009 the results were as follows for each governorate in each transplanting date the area is in Feddan (N.B Kafr Elsheikh_004 means kafrElsheikh governorate with its ΔEVI-parameter 0.04 and so on)

Table 4-9: Rice area in each governorate in each transplanting date

| Date | Kafr Elsheikh_004 | Behera_007 | Daq_005 | Gharbeya_005 | Sharqeya_005 | Dumyat_004 | Total |
|---|---|---|---|---|---|---|---|
| 15-Apr | 10600 | 4400 | 11300 | 7200 | 5500 | 2300 | 41300 |
| 23-Apr | 1300 | 1800 | 300 | 100 | 00 | 700 | 4700 |
| 1-May | 1900 | 19200 | 18300 | 19700 | 16700 | 3500 | 79300 |
| 9-May | 8100 | 700 | 9000 | 1100 | 16600 | 500 | 36000 |
| 17-May | 71700 | 4000 | 68100 | 15900 | 52100 | 1700 | 213500 |
| 25-May | 59300 | 2900 | 115900 | 11700 | 42800 | 3600 | 236200 |
| 2-Jun | 102900 | 37300 | 119100 | 29600 | 53100 | 14300 | 356300 |
| 10-Jun | 36600 | 43500 | 38900 | 23200 | 29300 | 11300 | 182800 |
| 18-Jun | 25500 | 58300 | 19600 | 34800 | 31300 | 4800 | 174300 |
| 26-Jun | 3000 | 27100 | 41500 | 31200 | 99700 | 3100 | 205600 |
| 4-Jul | 2800 | 23500 | 21500 | 14000 | 28400 | 500 | 90700 |
| 12-Jul | 2200 | 4300 | 4400 | 2600 | 8600 | 1000 | 23100 |
| 20-Jul | 1800 | 500 | 1500 | 200 | 1000 | 700 | 5700 |
| 28-Jul | 2100 | 400 | 800 | 100 | 800 | 800 | 5000 |
| 5-Aug | 3200 | 1300 | 800 | 800 | 100 | 900 | 7100 |
| 13-Aug | 0 | 0 | 0 | 0 | 0 | 0 | 0 |
| 21-Aug | 4500 | 600 | 1400 | 400 | 600 | 1600 | 9100 |
| | | | | | | | |
| Total | 337500 | 229800 | 472400 | 192600 | 387100 | 51300 | |

**Total 2009= 1670700 Feddan**

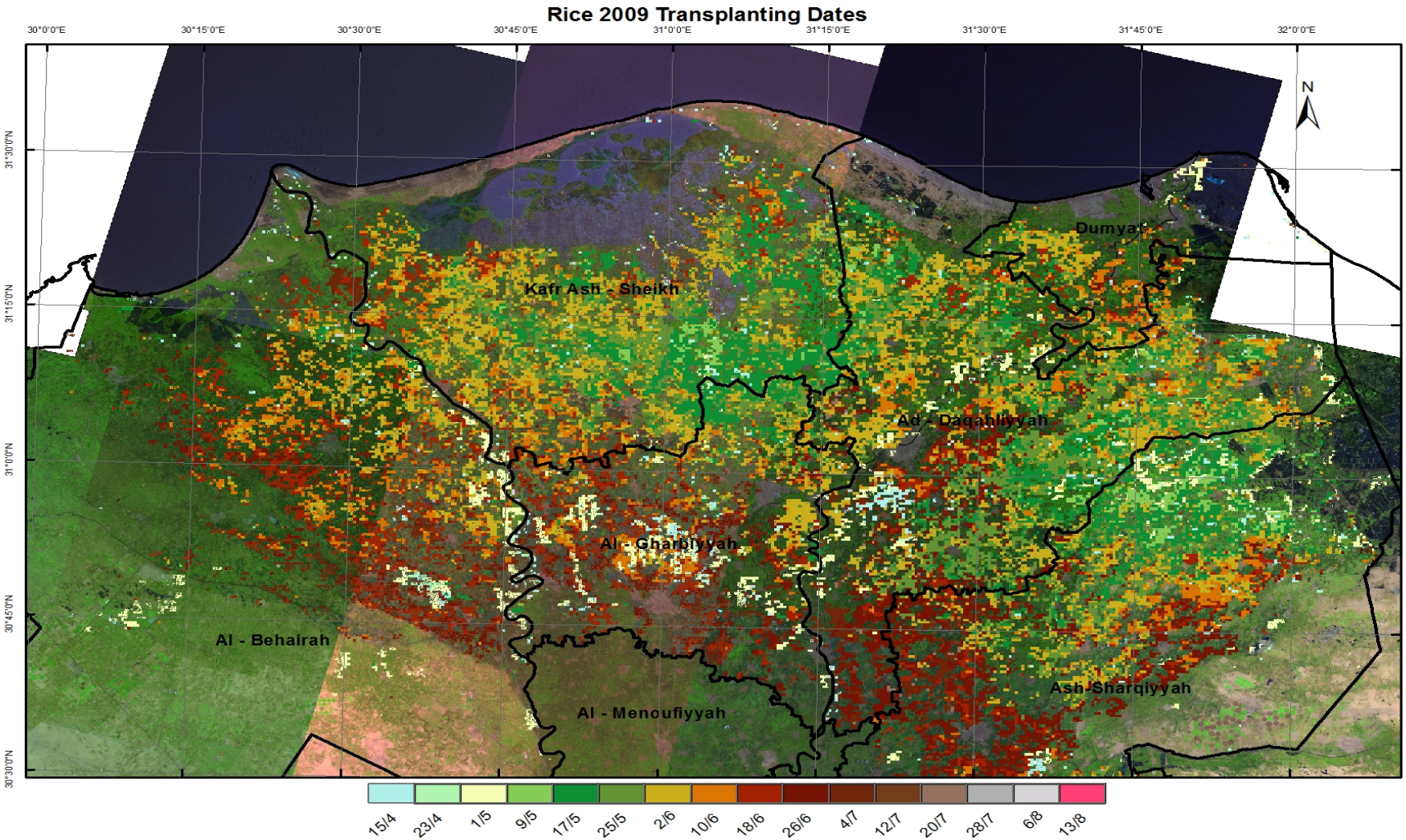


Fig 4-9: Output of the Rice area mapping Algorithm applied in 2009 for the Delta Region (Rice areas and transplanting dates)

# Chapter 5

# Advantages of the Rice Mapping Algorithm over the Traditional Supervised Classification Approach

## 5.1 The Traditional Approach of Rice Mapping

Another way of rice mapping that can be implemented other than the utilization of this research developed algorithm is the conventional supervised classification. In the conventional supervised classification, the priori knowledge of land types present is required. The collection of representative training samples of each type is vital. The required training sample size should be at least 30 times the number of the targeted land cover classes. These training samples should be distributed in different geographic locations in the scene in order to reflect the variability of the classes (Mathur, 2007). These samples are then used to train the chosen classifier. By applying some set of classification rules (depending on the classifier used), each other pixel in the satellite image is classified accordingly. The planning and collection of the training samples requires money and effort.

In order to compare the satellite imagery price required to run the developed algorithm with potential satellite imagery that can be used with the conventional supervised classification approach a thorough study of potential satellites was performed.

Satellites differs in collecting the imagery on a routine bases as they orbit the earth or not. For example, there are satellites that routinely collect imagery while they are orbiting like

MODIS, LANDSAT TM whereas other satellites collect images only when an order of collecting imagery is triggered; thus an order should be placed in advance for the satellite to collect imagery. This second type of satellites includes SPOT 5, Rapideye, and worldview 2. A study of these satellites characteristics namely MODIS, LANDSAT TM, SPOT 5, Rapideye and Worldview 2 was performed. The way to get their imagery was investigated. The spatial, spectral, temporal, resolution of each satellite was examined beside the swath width, the scenes required to cover the delta, and total price. Table 5-1 summarizes the main characteristic of those satellites and the requirements to cover the delta once.

From Table 5-1 it can be seen that as the spatial resolution increase the scene area coverage of the satellite decrease. For example MODIS with 500m resolution has an 1100 Km * 1100 Km scene area. This can cover the whole delta area in less than one scene. For LANDSAT with a 30 m resolution it requires two shifted along the track scenes to cover the delta region each with 170 km north-south by 185 km east-west dimensions. But for SPOT with 10m resolution it requires a 12 scene 60km * 60Km each to cover the delta region as shown in Fig 5-1.

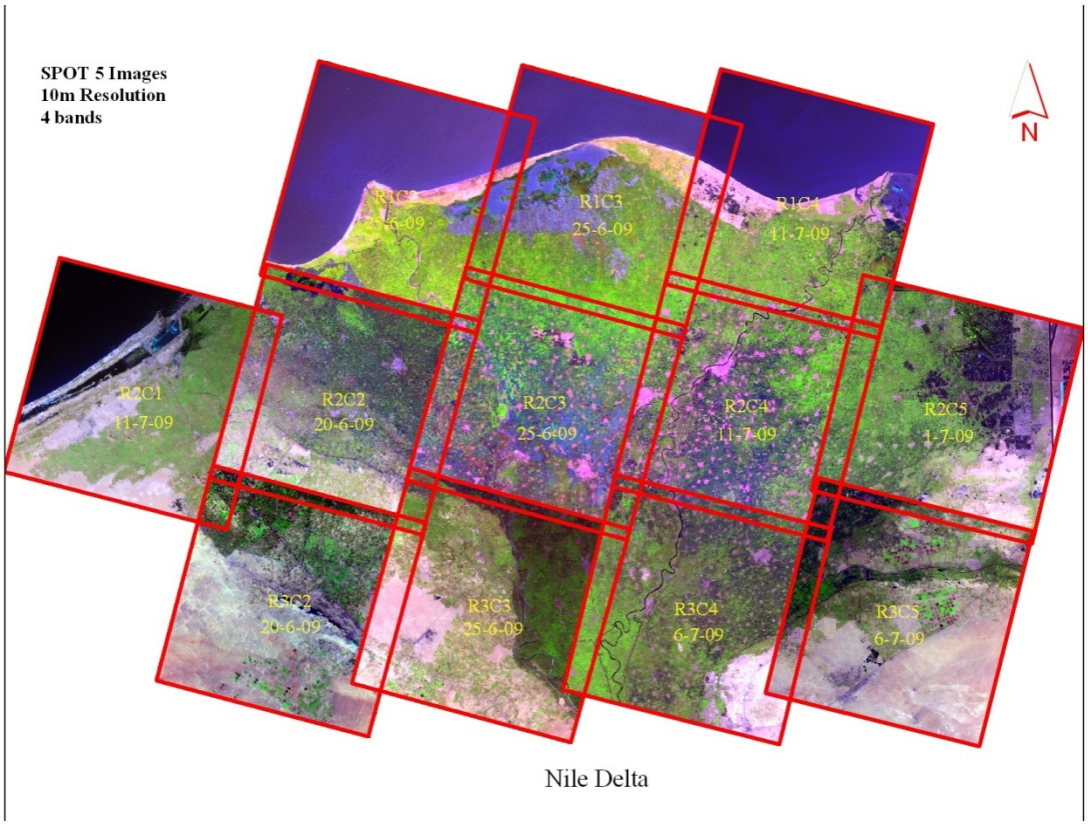


Fig 5-1: SPOT 5 scenes required to cover Delta region

For the Rapideye and worldview2 satellites, images of the delta area (30,000 $Km^2$) can be ordered on an area basis not on a scene bases like the previous satellites. This will provide more flexibility in exactly ordering the required area to be covered. For worldview 2 with a 60 cm resolution 8 band imagery the required delta area will cost 7,350,000 L.E as the $Km^2$ costs 245 L.E. The comparison of worldview2 cost to other satellites is shown in Fig 5-2. Commercial satellite imagery companies require some rules to be met when placing an order for buying their satellite imagery.

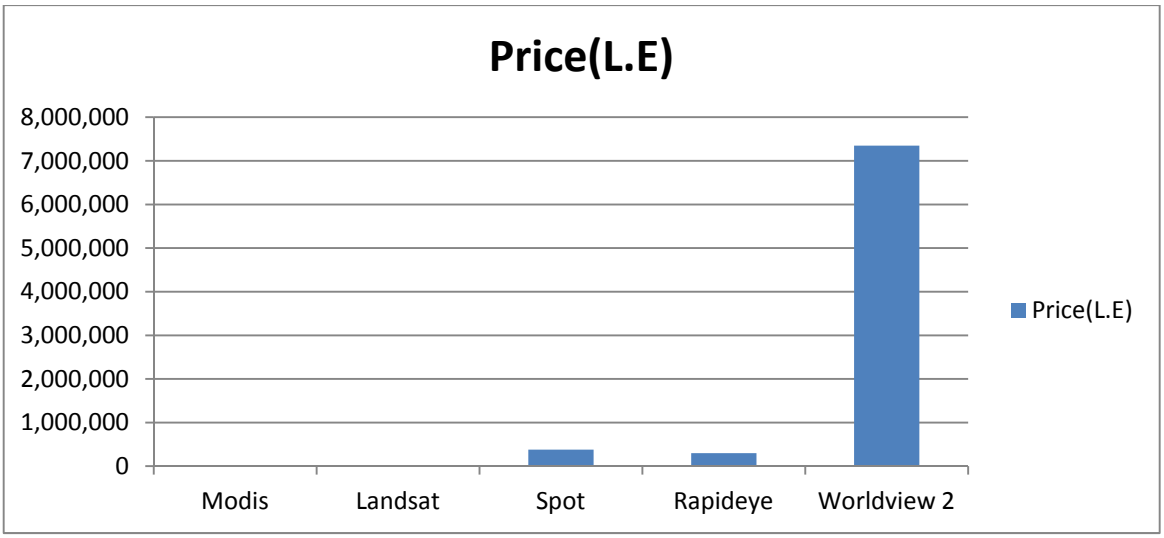


Fig 5-2: Worldview 2 cost compared to other satellites to cover Delta

By examining the potential satellites that can be used for rice mapping in Egypt and these rules. To image the whole delta once we need 12 SPOT scenes which will require tasking the satellite to image the delta with a cost of about 380,000 L.E. For Rapideye the cost to cover the delta only once is 300,000 L.E compared to just about 25,000 L.E for LANDSAT TM and getting MODIS imagery free of charge as shown in Fig 5-3.

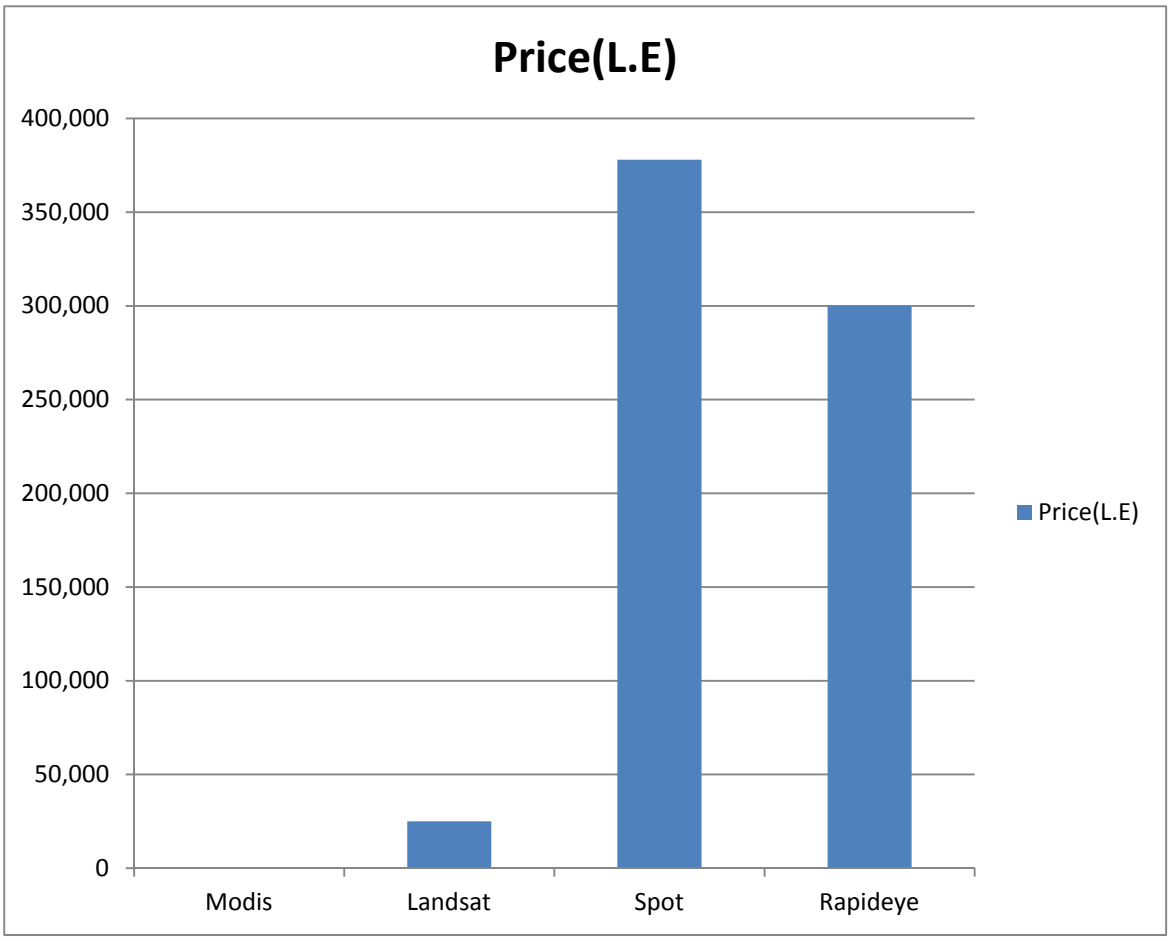


Fig 5-3: Price of potential satellite imagery to cover Delta

| Satellite Name | Category | Bands | Band Name | Bandwidth (nm) | Spatial Resolution (m) | Scene dimensions (Km) | Revisit time (days) | Delta coverage scenes or area | Price (L.E) | Total Price |
|---|---|---|---|---|---|---|---|---|---|---|
| MODIS | Coarse resolution | | | | | 1100 *1100 | Twice per day (Terra, Aqua) | 1 | Free | Free |
| | | 1 | Red | 620 - 670 | 250 | | | | | |
| | | 2 | Near Infra Red (NIR) | 841 - 876 | 250 | | | | | |
| | | 3 | Blue | 459 - 479 | 500 | | | | | |
| | | 4 | Green | 545 - 565 | 500 | | | | | |
| | | 5 | Short Wave Infra Red (SWIR 1) | 1230 - 1250 | 500 | | | | | |
| | | 6 | Short Wave Infra Red (SWIR 2) | 1628 - 1652 | 500 | | | | | |
| | | 7 | Mid Infra Red (MIR) | 2105 - 2155 | 500 | | | | | |
| Landsat | Mid resolution | | | | | 170 km north-south by 185 km east-west | 16 days | 2 | Partially | 25,000 |
| | | 1 | Blue | 450-520 | 30 | | | | | |
| | | 2 | Green | 520-600 | 30 | | | | | |
| | | 3 | Red | 630-690 | 30 | | | | | |
| | | 4 | Near Infra Red | 760-900 | 30 | | | | | |
| | | 5 | SWIR 1 | 1550-1750 | 30 | | | | | |
| | | 6 | Thermal | 10400-12500 | 120 | | | | | |
| | | 7 | Mid Infra Red (MIR) | 2080-2350 | 30 | | | | | |
| | | | | | | | | | | |
| SPOT | Mid resolution | | | | | 60*60 | 2-3 days | 12 | 31500 | 378,000 |
| | | 1 | SWIR | 1580-1750 | 10 | | | | | |
| | | 2 | NIR | 780-890 | 10 | | | | | |
| | | 3 | RED | 610-680 | 10 | | | | | |
| | | 4 | Green | 500-590 | 10 | | | | | |
| | | | | | | | | | | |
| Rapideye | Mid resolution | | | | | 24*24 area based | Daily | 30000Km$^2$ | 10/Km$^2$ | 300,000 |
| | | 1 | Blue | 440-510 | 5 | | | | | |
| | | 2 | Green | 520-590 | 5 | | | | | |
| | | 3 | Red | 630-685 | 5 | | | | | |
| | | 4 | Red Edge | 690-730 | 5 | | | | | |
| | | 5 | NIR | 760-850 | 5 | | | | | |
| | | | | | | | | | | |
| Worldview 2 | Very high resolution | | | | | 16.4*16.4 area based | Daily | 30000 Km$^2$ | 245/km$^2$ | 7,350,000 |
| | | 1 | Coastal | 400-450 | 2 | | | | | |
| | | 2 | Blue | 450-510 | 2 | | | | | |
| | | 3 | Green | 510-580 | 2 | | | | | |
| | | 4 | Yellow | 585-625 | 2 | | | | | |
| | | 5 | Red | 630-690 | 2 | | | | | |
| | | 6 | Red Edge | 705-745 | 2 | | | | | |
| | | 7 | Near - IR 1 | 770-895 | 2 | | | | | |
| | | 8 | Near - IR 2 | 860-1040 | 2 | | | | | |

Table 5-1: Potential Satellites to cover Delta region of Egypt for the conventional supervised classification approach

Xiao states that rice mapping with the conventional supervised approach is assigned with medium or high resolution satellite imagery (2005). Thus the least expensive to cover the delta once is purchasing LANDSAT TM images which will cost about 25,000 L.E. Although starting from June 2013 the new LANDSAT 8 (30 m) freely available imagery could also be used, still the selection of the imagery acquisition date appropriate to run the supervised classification is challenging. In addition, the collection of representing training samples is indispensable.

### 5.2 Key Advantages of the Rice Mapping Algorithm

The key advantages of the new developed rice-mapping algorithm over the conventional supervised classification approach can be summarized in the following points

1- No training samples are required
2- The satellite imagery used are free or already available
3- The classification of the key land covers: water, urban, desert and vegetation is obtained
4- MODIS imagery provides information throughout the rice planting season
5- The probable rice transplanting dates of each rice pixel is identified
6- The developed algorithm steps were modeled in ERDAS imagine remote sensing software. Thus the rice mapping application is performed in a semi-automated approach by just running the developed ERDAS models
7- The rice mapping occurs for the 8 day image interval thus, new transplanting rice fields can be mapped for every time interval
8- The early mapping of rice fields can help in rice yield estimate

9- Historical records of MODIS imagery are available since 2002, enabling the examination of the inter-annual variation in rice planting areas.

10- The inter-annual variation in the probable transplanting date for each rice field in the past 10 years can be calculated

11- How many times each field was planted rice in the past ten years can be determined(areas of persistent rice planting in violation of MWRI regulations can be mapped)

12- Knowing how many times each field was planted rice in the past ten years can help in predicting future planted rice field

# Chapter Six

# Summary, Conclusions and Recommendations

## 6.1 Summary

In this research a rice-mapping algorithm was developed. The algorithm consists of two modules. The first module utilizes the coarse imagery MODIS to study the dynamics of vegetation indices LSWI, EVI, and NDVI. The most differentiating feature of rice is being flooded during transplanting. In this period the LSWI (moisture sensitive) will temporarily exceed or approach EVI and/or NDVI (Greenness sensitive). In order to reflect this behavior, a Δ-parameter was introduced. Utilizing known rice fields the relation between LSWI, EVI and NDVI was studied and the Δ-parameter as a best fit for each rice-growing region was identified. The second module utilizes fine resolution LANDSAT imagery for arable land mapping. This was achieved through building a decision tree classifier that classifies imagery to main land covers, namely: urban, desert, vegetation and water. The non-vegetation area is then used for MODIS rice area refinement.

## 6.2 Conclusions

This research findings show that an economic remote sensing based rice mapping algorithm was developed. MODIS (Fine temporal resolution) free imagery with 500 m resolution can be used for rice mapping. This can be achieved by studying the relation between the land surface water index (LSWI), normalized difference vegetation index (NDVI), and enhanced vegetation index (EVI) indices dynamics throughout the rice

planting season. This can capture the most differentiating feature of rice (being flooded in the transplanting period). Rice can be mapped following the criteria of LSWI is temporarily greater than or approaches EVI or NDVI in the period of rice transplanting (LSWI > EVI or LSWI > NDVI).However, this criterion is modified by introducing Δ-parameter that is a best fit of each rice growing region. Thus rice mapping criteria adopted is LSWI + Δ > EVI or LSWI + Δ > NDVI. Novel vegetation versus non-vegetation module was developed. The LANDSAT (Fine spatial resolution) imagery (Free starting from June 2013) can be used for mapping main land covers namely: water, urban, desert, and vegetation. The blending of vegetation versus non-vegetation module with fine spatial resolution imagery can enhance the accuracy of rice mapping from MODIS. This is done by masking out non-vegetation areas within each MODIS pixel that was mapped from LANDSAT imagery and the veg-non-veg module. This decreases the major shortcoming of the mixed pixel dilemma occurring with MODIS especially in heterogeneous areas. The spatial distribution of rice areas and rice transplanting dates can be achieved.

The application of the rice-mapping algorithm to delta Egypt was carried out. The major land types in the Delta region; namely vegetation, (urban or bare land), desert and water can be discriminated by using the veg-non-veg developed module utilizing LANDSAT Tm imagery. The validation of this module with 1000 randomly selected points against very high resolution imagery (60 cm) in the east delta region showed an overall accuracy of 90.6%. This can then be used for rice mapping refinement. The utilization of the freely available MODIS imagery with its frequent revisit time for rice mapping in Egypt is feasible. The TM tuning resulted in a root mean square error =

56000 feddan. The application of the rice-mapping algorithm in year 2009 showed that the total rice planted area was 1670700 Feddan. About 82% of that area was transplanted from Mid-May to Mid-July. With the highest transplanting occurring in the period from 2 to 10 June. Furthermore, the most critical imagery availability dates in order for the algorithm to well function in Egypt are from Mid-May until Mid-July. The Δ-parameter for the six major rice-planting governorates was calculated. It was found that the Δ-parameter differs if EVI or NDVI will be used. The Δ-EVI parameter for Kafrelsheikh and Dumyat was found to be 0.04. Daqehleya, Gharbeya and Sharqeya Δ-parameter was estimated at 0.05. While Behera governorate Δ-parameter was estimated to be 0.07.

The Δ-NDVI parameter for KafrElsheikh was 0.174, for Dumyat was 0.178, for Sharqeya was 0.18, for Gharbeya was 0.197, for Behera was 0.23, and for Daqhleya the Δ-NDVI parameter was 0.155.The application of the proposed rice-mapping algorithm can help MWRI in the early identification of fields planted with rice in violation of MWRI regulations. The MWRI can then take prompt actions dealing with these violations.

The major advantages of the developed rice mapping algorithm over the traditional supervised classification approach are i) No training samples are required every year (saving money and time and protecting MWRI employees from being harassed and attacked by farmers) , ii)The probable rice transplanting dates of each rice pixel is identified, iii) the developed mapping algorithm is modeled to be semi-automated, iv) it can be applied on historical imagery without requiring the presence of training samples. However, the main limitation of the proposed approach is that the rice area is identified after the flooding occurs. It would have been much more helpful to be

able to predict the areas prepared for rice transplanting before the flooding takes place. This may be a very interesting point for future research.

## 6.2 Recommendations

- Investigating the possibility to use the reflectance of prepared rice fields for rice mapping before flooding takes place
- The vegetation versus non-vegetation module used available LANDSAT TM imagery. Thus it is strongly recommended to test the usage of LANDSAT 8 free imagery (available from June 2013) to update the output of the vegetation versus non-vegetation module.
- The MODIS 8 day product was used in the algorithm. Investigation of the usage of daily MODIS imagery is recommended as it could improve the identification of the transplanting date.
- Testing the usage of other water sensitive indices in the rice mapping algorithm
- Testing the ability to classify the rice mapped according to its variety
- Examine the inter-annual variation in rice areas in the last ten years by running the algorithm on MODIS historical imagery

# References,


Abd-El-Hai M., (2002).Rural Non-farm EmploymentWorkshop. Current and emerging issues for economicanalysis and policy research CUREMIS II NENA. FAO.INP.

AQUASTAT database,FAO. 2013. Food and Agriculture Organization of the United Nations (FAO). Website accessed on [28/01/2013 14:39]

Boschetti M.,Stroppiana D., Brivio P. A., Bocchi S., (2009), Multi-year monitoring of rice crop phenology through time series analysis of MODIS images, *International Journal of Remote Sensing*,Vol. 30, No. 18, 4643–4662

Bouvert A.,Toan T., Lam-Dao N., (2009), Monitoring of the Rice Cropping System in the Mekong Delta Using ENVISAT/ASAR Dual Polarization Data, *IEEE Transactions on Geoscience and Remote sensing*, Vol. 47, No. 2,

Bridhikitti A., Overcamp T., (2012), Estimation of Southeast Asian rice paddy areas with different ecosystems from moderate-resolution satellite imagery, Agriculture, Ecosystems and Environment 146 , 113– 120

CAPMAS.2013, Egypt in Figures, water resources, Central Agency for Public Mobilization And Statistics CAPMAS report 2013

Cheng Q., Huang J., Wang R., (2004) Assessment of rice fields by GIS/GPS-supported classification of MODIS data,*J Zhejiang Univ SCI 5(4)*:412-417

Chakraborty M.,Panigrahy S., Sharma S. A., (1997), Discrimination of rice crop grown under different cultural practices using temporal ERS-1 synthetic aperture radar data,ISPRS Journal of Photogrammetry & Remote Sensing 52 : 183-191

Doss M., Milne G., (2001). Water as an Economic good: an approach to the Egyptian economy, the BeijerWorkshop on "Property Rights Structures and Environmental ResourceManagement" Egypt, March 2001

Hobbs, S., Ang, W., &Seynat, C. (1998). Wind and rain effects on SAR backscatter from crops. *EUROPEAN SPACE AGENCY-PUBLICATIONS-ESA SP, 441*, 185-190.

Langley SK, Cheshire HM, Humes KS (2001) A comparison of single date and multitemporal satellite image classifications in a semi-arid grassland.*Journal of Arid Environment 49*:401–11.

Ling F., Wang X., Shi X., (2005), A processing method for rice crop inventory using multi-date ENVISAT-1 ASAR data, Proceedings of SPIE, the International Society for Optical Engineering, International conference on space information technology, Wuhan , CHINA , vol. 5985 (2)

A.Mathur and G.Foody, 2007, Crop classification by Support vector machine with intelligently selected training data for an operational application, *International Journal of Remote sensing Vol29,*No8 2227-2240

Nordberg ML, Evertson J (2003) Vegetation index differencing and linear regression for change detection in a Swedish mountain range using Landsat TM and ETM+ imagery. *Land Degradation & Development 16*:139–149.

Ozkuralphi I., (2007), Monitoring crop growth in rice paddies in the Thrace-Meric basin with multitemporal RADARSAT-1 Satellite images, ISPRS Commission VII WG2, WG7

Sakamoto T., (2005), A crop phenology detection method using time-series MODIS data,*Remote Sensing of Environment 96*, 366 – 374

Sun H. et al., (2009), Mapping paddy rice with multi-date moderate-resolution imaging spectroradiometer (MODIS) data in China, *J Zhejiang UnivSci A , 10(10)*:1509-1522

Wang X., Wang Q., Ling F., Chen H., Quegan S., (2008), Backscatter change index of ENVISAT ASAR data for rice field mapping in Fuzhou, Fujian province, Proc. Dragon 1 Program Final Results 2004–2007, Beijing, P.R. China

Xiao, X., Boles, S., Frolking, S., Salas,W., Moore, B., Li, C., et al. (2002).Observation of flooding and rice transplanting of paddy rice fields at thesite to landscape scales in China using VEGETATION sensor data. *International Journal of Remote Sensing, 23*, 3009– 3022

Xiao X., Boles S., Frolking S., Li C., Babu J., Salas W., Moore B., (2006), Mapping paddy rice agriculture in South and Southeast Asia usingmulti-temporal MODIS images, *Remote Sensing of Environment 100*, 95 – 113

Xiao X., (2005),Mapping paddy rice agriculture in southern China using multi-temporal MODIS images, *Remote Sensing of Environment 95*, 480–492

Xie Y., ShaZ., Yu M., (2008), Remote sensing imagery in vegetation mapping: a review, *Journal of plant ecology*, vol 1, no 1

Yuan Z., Wang C., Wu J., Qi J., Salas A., (2009), Mapping paddy rice with multitemporal ALOS/PALSAR imagery in southeast China, *International Journal of Remote Sensing, vol 30, no 23*